SPECTRUM SENSING ALGORITHMS FOR COOPERATIVE COGNITIVE RADIO NETWORKS

A THESIS IN ELECTRICAL ENGINEERING

Master of Science in Electrical Engineering

Presented to the faculty of the American University of Sharjah
College of Engineering
in partial fulfillment of
the requirements for the degree

MASTER OF SCIENCE

by
YASMIN ADEL HASSAN
B.S. 2008

Sharjah, UAE
May 2010

SPECTRUM SENSING ALGORITHMS FOR COOPERATIVE COGNITIVE RADIO NETWORKS

Yasmin Adel Hassan, Candidate for the Master of Science Degree

American University of Sharjah, 2010

ABSTRACT

In the past few years, there have been remarkable developments in wireless communication technology, leading to a rapid growth in wireless applications. However, this dramatic increase in wireless applications is severely limited by bandwidth scarcity; a fundamental resource for communications. Traditionally, fixed spectrum assignments are used in which frequency bands are statically assigned to licensed users. The static spectrum allocation fails to provide vacant spectrum bands to new coming users and services. Hence, a new communications and networking paradigm based on dynamic spectrum allocation has emerged, namely cognitive radio system.

In cognitive radio networks, spectral utilization is improved by allowing unauthorized (secondary) users to regularly sense the radio spectrum and opportunistically use frequency bands not utilized by licensed (primary) users. Primary users have higher priority than secondary users; therefore, secondary users need to utilize idle spectrum holes without causing harmful interference to primary users. In order to achieve minimum level of interference to primary users, efficient spectrum sensing techniques need to be implemented.

Spectrum sensing is one of the main challenges in opportunistic spectrum usage, since it is responsible for providing efficient and fair spectrum access and scheduling

among licensed and unlicensed users. Cooperation between cognitive radio users has been proposed in the literature to overcome spectrum sensing challenges by providing spatial diversity. Both centralized and decentralized cooperative spectrum sensing systems have been implemented to enhance detection capability of cognitive radio networks.

In this work, we formulate the cooperative spectrum sensing process as a pattern recognition problem, where a centralized node classifies the target spectrum into two classes: busy (presence of signal) or vacant (absence of signal). The classifier is designed to identify white spaces in the spectrum while minimizing interference with licensed primary users and maximizing spectral utilization in environments exhibiting shadowing and fading effects. Polynomial classifiers were proposed in this work as classifier models, in which first and second order expansions are investigated.

Feature extraction stage consists of two spectrum sensing techniques: parametric and non-parametric. In nonparametric detection algorithms, such as energy detection and autocorrelation, the cognitive network does not have a priori knowledge on the primary users' signals. On the other hand, in parametric detection, cyclic features characterizing primary signals and prior knowledge of synchronizing preamble patterns are utilized. The parametric detection schemes include coherent detection and cyclostationary feature detection.

Extensive simulations were performed to design, model, and evaluate the cooperative classifier system, when both parametric and nonparametric features are used. In nonparametric spectrum sensing, simulations demonstrate the superior performance of autocorrelation detection scheme over energy detection. Moreover, simulations of parametric spectrum sensing indicate that cyclostationary feature detection outperforms coherent detection. Finally, it was shown that parametric sensing schemes yields a superior performance over nonparametric sensing schemes when implemented under same conditions.

CONTENTS

LIST OF FIGURES

LIST OF TABLES

LIST OF ABBREVIATIONS

ANN	-	Artificial Neural Network
AWGN	-	Additive Wide Gaussian Noise
BC	-	Binomial Classifier
BPSK	-	Binary Phase Shift Keying
CAF	-	Cyclic Autocorrelation Function
CD	-	Coherent Detection
CFD	-	Cyclostationary Feature Detection
CR	-	Cognitive Radio
DS-SS	-	Direct Sequence Spread Spectrum
FCC	-	Federal Communications Commission
FFT	-	Fast Fourier Transform
FH-SS	-	Frequency Hopping Spread Spectrum
LC	-	Linear Classifier
MISO	-	Multiple Input Single Output
PAM	-	Pulse Amplitude Modulation
PSK	-	Phase Shift Keying
ROC	-	Receiver Operational Characteristics
SCD	-	Spectral Correlation Density
SLS	-	Square Law Detection
SLC	-	Square Law Combining
TDMA	-	Time Division Multiple Access
WRAN	-	Wireless Regional Area Network

ACKNOWLEDGEMENTS

First of all, thanks to ALLAH for sustaining me throughout my Master's journey. It has been a long journey for me and also for many people who have supported me to accomplish my achievements in this thesis. Foremost, I am very grateful to have two of the most knowledgeable and inspiring advisors that I could ever wish for, Professors Mohammed El-Tarhuni and Khaled Assaleh. I would like to thank my mentor Dr. El-Tarhuni for joyfully providing me with guidance, motivation, and directions to conduct a high quality research. His teaching formally introduced me to the field of wireless communications, providing me with solid background in my work in cognitive radios. I have not only benefited from his broad knowledge in digital and wireless communications, but also from his research techniques and punctuality. I was also fortunate to have Dr. Assaleh as my advisor, who introduced me to the field of pattern recognition, and patiently taught me the fundamentals of this area. I would like to thank him for being there to answer my inquiries and offer new techniques to achieve my objectives. Without his broad knowledge and continuous guidance, this thesis wouldn't be in the shape it is.

I am also grateful to the graduate committee, Dr. Mohammed Hassan and Dr. Muhieddin Amer for the time and effort they spent in reading my report and providing me with their valuable comments. I would like to take this opportunity to thank the Electrical Engineering department at AUS for granting me the assistanceship to peruse my Masters degree. I would like to further thank all my professors for their unconditional guidance, support and encouragement during the past two years.

Special thanks go to my colleagues and best friends, Omniyah Noory and Yara Fayyad, who have shared the majority of my time for two full years. I have spent with them great times in and out of our lab, during which I managed to annoy or disturb them one way or another. Their understanding, support and constant encouragement have made my Masters experience very enjoyable.

Lastly, but most importantly, no words can express my deepest appreciation to my parents and brothers who have been next to me in this journey all the way. Thank you my brothers, Ahmed and Mostafa, for making me realize my capabilities and potentials, pushing me towards my goal. To my Mom and Dad: you are the reason for

all what I'm today and all what I have accomplished in my life. Thank you for your endless love, support, sacrifice, care and sincere prayers and providing me with foundations to always be able to fall back on.

To my truly loved parents and bothers,

for your endless love, care, and unwavering faith in me

CHAPTER 1

INTRODUCTION

There has been a rapid development in wireless communication applications due to significant technological advancements in the field. The explosion of wireless applications can be envisioned in mobile communications, wireless PANs/LANs/MANs, Wi-Fi, TV broadcast services, etc. This enormous growth in the telecommunication field resulted in severe shortage in the available radio frequency spectrum. In traditional spectrum allocation schemes, fixed frequency bands are statically assigned to licensed users. Having most of the available spectrum statically allocated, frequency regulation bodies fall short to provide vacant bands to newly developed wireless services. On the other hand, spectrum occupancy measurements have shown that some licensed bands are significantly underutilized. For example, the Spectral Policy Task Force reported that radio channels are typically occupied 15% of the time with a peak occupancy reaching 85% [1]. This indicates that spectrum limitations occur due to the inefficient static allocation techniques, rather than physical spectrum scarcity. Therefore, the underutilization of available spectrum resources has led regularity bodies to urge the development of dynamic spectrum allocation paradigms, called cognitive radio (CR) networks.

CR networks utilize dynamic spectral allocation to overcome spectrum scarcity. In CR technology, unauthorized (secondary) users are allowed to share the spectrum originally assigned to authorized (primary) users. In other words, frequency bands that are legally assigned to primary users are exploited by secondary users when the primary users are idle. However, primary users have the right to occupy their assigned bands whenever needed. Consequently, a CR network should be aware of the variations in the surrounding environment and adjust its operating parameters accordingly. In order to standardize the deployment of CR networks, the IEEE 802.22

Working Group was formed in 2004. The working group has been developing a standard for a wireless regional area network (WRAN) with CR based radio interface for operation in licensed bands. The operating bands to be exploited by WRANs are the ones currently licensed for analog and digital television broadcasting and wireless microphones [2].

Secondary users in CR networks are restrained by the condition of causing no harmful interference to primary users. Hence, they need to employ efficient spectrum sensing techniques that ensure the quality of service for primary users and exploit all dynamic spectrum sharing chances. That is to say, in order to facilitate dynamic spectrum access in licensed bands, effective spectrum sensing algorithm needs to be developed whereby high reliability along with effective utilization is achieved. According to the decision made by the spectrum sensing method, CR devices will dynamically alter their operating frequency, transmission power, modulation, etc. By being able to successfully identify spectrum holes and efficiently allocate the available spectral resources, CR network can provide different services to its users. However, it needs to achieve high detection probability to keep a minimum level of interference to coexistent primary users. For example, Table 1.1 illustrates the requirements for cognitive users for the WRAN standard [1][2] . The requirements are provided for the different signal types targeted by the standard, which are analog and digital TV and wireless microphones. Moreover, the standard identifies the channel detection time to be less than 2s; and the CR is required to achieve a detection probability of 0.9 with false alarm rate of 0.1. It can be noted that sensing cognitive user needs to operate under very low SNR values, which is an expected scenario in CR networks to provide protection to primary network.

Table 1.1. Receiver parameters for IEEE 802.22 WRAN.

Parameter	Analog TV	Digital TV	Wireless Microphone
Detection probability	0.9	0.9	0.9
False alarm probability	0.1	0.1	0.1
Channel detection time	$\leq 2s$	$\leq 2s$	$\leq 2s$
SNR	1 dB	-21dB	-12dB

CR users sense the primary users' licensed channel, if a frequency band is occupied by primary user; it is called an active band. Otherwise, it is called an idle band. We also refer to the inactive bands by spectrum holes or white space, while the active bands are referred to by black spaces [3]. The spectrum sensing algorithm needs to classify the target frequency band into white or black spaces, where white spaces are proper candidates for spectrum allocation to CR users, and vice versa. Several spectrum sensing methods have been proposed in literature so far such as energy detection, coherent detection, cyclostationary feature detection, and autocorrelation detection [1][3][4][5][6][7][8][9][10][11][12]. Each secondary user senses the surrounding environment and uses one of the spectrum sensing methods to decide on spectrum vacancy. However, the received signal is usually affected by fading and shadowing effects, making it hard to obtain a reliable decision at a single receiver. To reduce the shadowing and fading impacts, cooperation between several CR users in making the spectrum availability decision has been proposed to exploit spatial diversity gain. Most of the prior works implement cooperative spectrum sensing via cooperative techniques such a maximum ratio combining, likelihood ratio test, or hard decision rules, such as AND logic operation and one-out-of-n rule.

In this work, we propose a novel cooperative spectrum sensing approach in CR applications. Specifically, we propose to utilize classification techniques used in pattern recognition applications to identify the white and black spaces in the spectrum. The proposed pattern recognition scheme represents a centralized cooperative CR network whereby the decision of spectrum availability is made at a central node (e.g. network base station) after collecting sensing information from all collaborating users. Sensing information is subjected to a classifier model that outputs a global decision. In this work, first and second order polynomial classifiers are used.

Various spectrum sensing techniques are implemented to provide informative features to the classifier about the surrounding environment. We categorize spectrum sensing methods into nonparametric (energy and autocorrelation detection) and parametric (coherent and cyclostationary). In nonparametric schemes, we investigate the performance of the simplest sensing technique with least computational complexity, namely energy detection. Features extracted via energy detection are attractive since they provide good performance when received signal level is high, while requiring no prior knowledge on primary signal parameters and have simple

implementation. When no prior information is available at the CR network and the received signal level is low, more discriminative features are needed for proper classification. This is achieved by adopting a nonparametric autocorrelation detection scheme. In this thesis, we compare the performance of the two nonparametric detection techniques as they are applied to the designed classifier.

Additionally, in parametric sensing we consider scenarios in which prior information about licensed users is available to the CR network. Knowledge of synchronizing preamble patterns is used in coherent detection. Moreover, modulation parameters of primary user's signals are utilized through cyclostationary feature detection. Once again, the extracted features by parametric sensing schemes are applied to the polynomial classifier for decision making.

This thesis is aimed to meet the following objectives:

- To design a cooperative spectrum sensing algorithm for cognitive radio networks using a polynomial classifier model to identify white spaces in the spectrum in a fading environment.
- To evaluate and compare the performance of parametric and nonparametric feature extraction techniques when applied to the classification system.

The intellectual contributions presented in this thesis can be summed up in the following points.

1. *Pattern recognition in signal identification:* We have addressed the problem of cooperative spectrum sensing in CR networks from a new perspective. White space identification was modeled as pattern recognition system, where the classifier's output score provides a centralized decision on spectrum vacancy. We performed the design, validation and evaluation of first and second polynomial classifiers as a classifier model.
2. *Nonparametric sensing*: We provided a comprehensive performance evaluation of nonparametric spectrum sensing schemes as they are applied in feature extraction. Received energy and autocorrelation were used to provide discriminative features to the classifier models. The system

performance was investigated under various operating conditions and in environments exhibiting shadowing and fading effects.

3. *Parametric sensing:* Extensive simulations were also performed to evaluate the performance of parametric spectrum sensing schemes, where carrier frequency and synchronization preamble patterns are assumed to be known at the CR network. Cyclostationary feature detection and coherent detection approaches were examined as feature extraction techniques. The overall parametric system performance was investigated. Thereafter, the performance of parametric and nonparametric schemes was compared.

4. In this thesis, we have applied a weighted soft decision rule, provided by the proposed classifier to both parametric and nonparametric feature extraction schemes. The model's weighting parameters are designed so that the contribution of cognitive users with lower reliability is suppressed and vice versa. The performance in terms of false alarm rate and detection probability under low SNR regimes has been thoroughly examined and analyzed.

The remainder of the thesis is outlined as follows. The background behind CR networks along with a review of current literature is presented in Chapter 2. A general background of pattern recognition systems and classifier models is also explained. In Chapter 3, the system model of the proposed classification algorithm is described, including the adopted network architecture, the performance metrics to be considered and the model design and estimation. Nonparametric spectrum sensing schemes are applied to the classifier model and their performance is evaluated in Chapter 4. Parametric sensing schemes are introduced and their performance is assessed in Chapter 5. Finally, conclusions are drawn and future work is discussed in Chapter 6.

CHAPTER 2

BACKGROUND

The background concepts of cognitive radio (CR) networks are presented in this chapter. Literature survey of different spectrum sensing techniques is presented, followed by the main challenges facing spectrum sensing in cognitive radio networks. An overview of radio propagation mechanisms in wireless environments and multipath fading channels is illustrated. Thereafter, a general background on the main considerations and steps of designing pattern recognition systems is given. Finally, some pattern recognition tools are presented including artificial neural networks and polynomial classifiers.

2.1 Cognitive Radios (CR)

Due to the increasing popularity of various wireless technologies, varying from voice only applications to multimedia type applications, the demand for more band width and higher data rates has increased. Most of the available wireless frequency spectrum is already assigned by spectrum regulation bodies, such as the Federal Communications Commission (FCC), to licensed primary users [4]. Although few unlicensed bands were allocated, commonly known as the industrial scientific and medical (ISM) bands, most of the frequency spectrum is licensed. Additionally, the available unlicensed band is already being filled up rapidly as the use of wireless devices in different applications increases. This has motivated innovative techniques to overcome the scarcity of the spectrum and enhance spectrum utilization rather than the current static spectrum allocation techniques.

Within the last decade, deployment of dynamic spectrum allocation systems was considered to address the spectrum scarcity problem, through the use of CR technology. CR is a radio system that is capable of sensing its operating environment

and dynamically utilizing the available radio resources [5][6]. The CR network should adapt to changing frequency usage within the target frequency band in order to make a productive usage of the spectrum. CR systems ultimately perform continuous spectral sensing in order to dynamically identify the unused spectrum holes, at which the primary users are idle, and utilize them. To understand the operation of cognitive radios, we define two types of spectrum users. Users of high priority or legacy rights to use the spectrum are called *primary users*. On the other hand, users with lower priority, who are not assigned a specific frequency band to operate at, are called *secondary users*. Secondary users also referred to as CRs, can only use the spectrum such that they do not cause interference to primary users. Consequently, whenever an activation of primary users is monitored, secondary users should vacate the occupied spectral segments, and hence the spectrum will be used conservatively in the favor of the primary user [7].

2.1.1 Cooperative Spectrum Sensing

A major requirement of CRs is the ability to successfully sense the surrounding environment and maximally utilize available bands. Further, secondary users should provide careful protection to primary users from interference resulting from the CR network operation. One approach of signal detection is based on local decisions made at each secondary user. If a priori information on primary user's signal is known by secondary users, coherent detection can be utilized to maximize the ability of the CR to detect the primary user. Coherent detection utilizes features such as synchronization messages, pilots, preambles, midambles, spectrum spreading sequences, etc. Preambles are synchronization patterns that are transmitted before each burst of bits, while midambles are transmitted in the middle of the time slot. When these patterns are known at the CR network, sensing is performed by correlating the incoming signal with the known patterns [8]. Coherent sensing based on pilot detection was implemented experimentally in [9]. Measurements indicate that coherent detection shows considerable reduction on sensing time required to achieve a certain detection level as compared to energy detection. However, it was shown that coherent detection is susceptible to synchronization error.

Another approach is based on cyclostationary detection which exploits cyclostationary features exhibited by the statistics of the primary signal.

Cyclostationary features are caused by the periodicity of the signal's statistics or may be induced intentionally to facilitate spectrum sensing [8]. In cyclostationary detection, the spectral correlation function (SCF) of the modulated signal is analyzed to differentiate between the case when signal is present and when noise only is present [10]. Cyclostationary feature detection is further discussed in Chapter 5. In orthogonal frequency division multiplexing (OFDM) systems, guard intervals are utilized to exploit cyclostationarity in spectrum sensing [11]. The cyclic prefix is not inserted in the OFDM guard interval which is used for detecting the incumbent primary signals. In this case, inter carrier interference (ICI) is avoided and circulant convolution is preserved using a scheme developed in [12]. Further, the OFDM waveform is modified in order to generate specific signatures at certain frequencies [13]. The cyclic features created by these signatures are then extracted via cyclostationary detection to achieve effective signal identification mechanism.

Although the above mentioned techniques provide good performance with accurate detection of primary signals, they require a priori information about the primary users. If this information is not available, energy and autocorrelation detection methods are considered as good alternatives. In this scenario, secondary users estimate the energy of the received signal and compare it to a threshold to decide if a signal is present of not. Although this is a simple technique, energy detector's performance is highly compromised due to noise uncertainty [7][14][15]. Experimental studies were performed to investigate spectrum sensing of weak signals in CR networks using energy detection [14]. The energy detection was both simulated and experimentally implemented in an indoor non-fading environment, in which three types of signals were sensed, purely noise, single tone and QPSK signals. The threshold was set based on the knowledge of noise variance and assuming a constant false alarm rate.

The detection performance of CR sensing is often compromised with destructive channel conditions like shadowing and fading, which are discussed in the next section. Under these conditions, it becomes difficult to differentiate between the existing weak primary signal attenuated by deep fading and the noise. This may cause the CR to decide to use the channel due to miss detecting the primary signal. Recently, collaborative sensing in CR networks has been proposed to exploit the spectrum efficiently while minimizing interference with primary signals [6][7][8][17][18][15].

In this case, several CR nodes utilize the spatial diversity provided by cooperative spectrum sensing to achieve better performance in fading environments. Moreover, cooperation between cognitive users can effectively solve the hidden primary problem [8].

Collaborative spectrum sensing is proposed in which each CR utilizes energy detection in making a decision on spectrum availability based on the noise level sensed at that receiver [6][14][17]. Thereafter, the decisions made by various CRs are exchanged among them, where a hard decision based on majority vote is performed at each CR. In [7], cooperation of cognitive users is performed utilizing a soft decision rule, in which a linear combination of received energies is used to make a decision. There are two approaches to collaborative sensing, which are centralized and decentralized sensing. In centralized sensing, a global decision is made at a centralized fusion center and broadcasted to all users in the network. Alternatively, in decentralized sensing, each CR makes a local decision, combines all received local decisions to make a global decision, and act accordingly [8].

Cooperative sensing with five users has shown an improvement of 36% in detection probability over single CR decision [11][9]. The impact of physical separation between CRs on cooperative multiuser network was also investigated [9]. It was found that as the level of correlation between cognitive users increases, the less the cooperation between them is effective. The performance of cyclostationary based spectrum sensing in multiple-antenna CR system was considered in [17]. Fusion rules such as maximum ratio combining, 1-out-of-*n*-rule, and comparison detection were compared for cooperative cyclostationary detection. It was found that maximum ratio combination performs the best among the three fusion rules studied.

Energy detection over fading channels was investigated in [15][13][16]. The false alarm and detection probabilities were derived, assuming the received signal follows a Nakagami distribution. Both square law combining (SLC) and square law selection (SLS) diversity methods were studied for independent and identically distributed (i.i.d.) fading channels as well as correlated channels. Spatial diversity provided by cooperative sensing has effectively improved systems performance. Moreover, when the correlation between the CRs diversity system decreases, detection probability for the same false alarm level increases.

2.1.2 Challenges of Spectrum Sensing

A key component in the operation of a CR network is spectrum sensing and being aware of the existence of primary signals in the target frequency band. Some of the challenges facing spectrum sensing in CR networks are discussed below.

2.1.2.1. Multidimensional Spectrum Sensing

There are different dimensions over which spectrum sharing can be implemented. Conventionally, spectrum sharing dimensions include frequency, time, space, and code [8]. In frequency sharing, the spectrum is divided into narrower bands that are not used simultaneously and hence some bands might be available for opportunistic sharing. However, the availability of certain parts of spectrum in time represents an opportunity in the time dimension. The space dimension is utilized when primary and secondary users share the same band at the same instant in time, taking advantage of propagation loss in space. Further, the code dimension is used when spread spectrum techniques are deployed. In these cases, the conventional energy detection techniques fail, since the energy of the received signal is being spread all over the spectrum. However, if the code dimension is implemented as part of spectrum sensing process, it could provide higher utilization opportunities.

Another dimension that can be added is the angle dimension, which is different from the space dimension. So far, most of the studies in the literature assumes that all users are transmitting everywhere in all directions [8]. However, advances in antenna designs enable primary and secondary users to send the signal in a narrow direction, considering the angle of arrival (AOA) of the received signal as additional dimension in spectral utilization. By utilizing AOA as additional dimension, a CR user can decide that a channel is idle at a specific instant of time in a known geographical area for a receiver with certain AOA.

2.1.2.2. Hardware Architecture

The sensing process can be performed using two architectures, namely single-radio and dual-radio. In the case of single-radio, each secondary user

uses the same radio chain for both spectrum sensing and signal transmission, i.e. part of the time is allocated for sensing and the rest for actual transmission [19][20]. On the other hand, the dual-radio structure uses two different radio chains, one for continuous spectral monitoring while the other one is dedicated for transmission and reception. The main disadvantage of the single-radio architecture is the decrease in the spectrum efficiency since part of the time slot is being used for sensing. Its main advantage, though, is its simplicity and the low complexity of the system as opposed to the dual-radio architecture. Although dual-radio architecture increases the power consumption and hardware cost, it offers high spectrum efficiency and sensing accuracy.

2.1.2.3. Spread Spectrum Primary Users

Primary users can send their messages over either fixed narrowband frequency channels or as spread spectrum signals. In spread spectrum, the signal energy is either spread over a very wide frequency band as in Direct Sequence Spread Spectrum (DS-SS) or sent over a narrow frequency that alters between different frequency channels as in Frequency Hopping Spread Spectrum (FH-SS). In FH-SS, the center frequency changes according to a pseudo random (PN) code. In this case, it becomes hard to detect the presence of the primary signal using energy detectors as the signal's power is distributed among a wide range of frequencies. On the other hand, if a priori information is known about the primary signal such as the PN code, energy detection can be used [18].

2.2 Wireless Propagation

The quality of wireless and mobile radio systems is affected by many factors including signal dispersion, operating frequency, attenuation, path obstructions, etc. Hence, in order for a realistic mobile system design and deployment, it is very important to distinguish the different features of mobile signal propagation in wireless environments. As opposed to reliable wired communication channels that are predictable and stationary, modeling of a radio channel is based on statistical and measurement characterization. An ideal radio propagation situation is a line of sight

(LOS) propagation in free space without any obstacles between transmitter and receiver. In reality, obstacles exist in the radio channel, resulting in different propagation mechanisms and losses to the radio waves.

2.2.1 Propagation Mechanisms

There are three propagation mechanisms that are used to describe radio propagation [21][23]:

2.2.1.1. Reflection

Reflection occurs when propagating electromagnetic waves impinge on obstructing objects that are larger than their wavelength. Such objects include the surface of the earth, walls of tall buildings, the ceiling, and the floor. Reflections of incident radio waves result in attenuation of the waves' strength, which depends on the frequency of operation, angle of incidence and the nature of the medium.

2.2.1.2. Diffraction

Diffraction of electromagnetic waves occurs more frequently and has higher impact on the incident wave in indoor applications than outdoors. Incident waves on sharp irregular edges of buildings, walls and other large objects act as a secondary source, which results in diffracted fields propagating into shadowed regions in which no LOS exists.

2.2.1.3. Scattering

Scattering of incident waves is caused by irregular objects with dimensions that are close to or smaller than the wavelength of the propagating wave, such as walls with rough surfaces, furniture, and vehicles. The incoming signal is hence scattered in all directions into several weaker signals reducing its power levels.

2.2.2 Propagation Loss

Another way to characterize radio propagation mechanism is by identifying the propagation loss in a channel which characterized by path loss, large scale fading and small scale fading. The path loss represents the average loss in the signal's strength

based on the distance between the two communicating terminals. The wireless signal variations within short transmitter- receiver distance are characterized by small-scale fading. On the other hand, large scale fading characterizes changes in the transmitter signal over large distance between transmitter and receiver. A discussion of the three mechanisms of propagation loss in a channel is given as follows:

2.2.2.1. Path Loss

The pass loss corresponds to the average signal's level loss over a wide range and is usually used to determine signal coverage in wireless networks. Path loss modeling relates the deterioration in signal strength to the macroscopic parameters, such as distance between two terminals, the carrier frequency, and the land profile. There is no unique path loss to describe radio propagation in all environments, since wireless communications span different environments. The simplest formula for the path loss propagation between two communicating ends separated by distance d is [21][22].

$$L_p = A + \gamma \log(d) \quad \text{(dB)} \tag{2.1}$$

where A and γ are referred to as propagation constants. Propagation constants are estimated empirically via propagation measurements and vary based on the considered environment. For example, Okumara-Hata models are developed for urban areas and other models are developed for suburban and open areas.

2.2.2.2. Large Scale Fading

The path loss determines the deterioration in the signal level due to travelling a distance d ; however, practically the received signal strength at the same distance from the transmitter varies because of the environment and surroundings. Hence, the value of the path loss determined by (2.1) represents the mean or average value of the signal strength estimated at a receiver located at distance d from the transmitter. This long term spatial and temporal variations of the signal's strength are referred to as large scale fading or shadow fading. The fluctuations of the received signal level around the mean value are caused by variation in propagation conditions, due to buildings, walls and other obstacles in a relatively small area. In this case, the path loss

defined earlier needs to be modified to include this effect by adding a random variable X with a distribution that depends on the fading component:

$$L_p = A + \gamma \log(d) + X \quad \text{(dB)} \qquad (2.2)$$

Experiments and simulations indicate that path loss obeys a log-normal distribution with a mean $\bar{x} = A + \gamma \log(d)$ in decibels; representing the average received signal level. The random variable X has a variance ${\sigma_x}^2$ that statistically describes the path loss model for an arbitrary location with a specific distance d. The variance ${\sigma_x}^2$ takes values between 4 and 12 dB according to the propagation environment [21].

2.2.2.3. Small Scale Fading

Small scale fading represents the fast fluctuation in the signal strength due to the scattering of the signal by objects near the transmitter. It also occurs as a result of the movement of the transmitter, receiver or objects surrounding them. Two factors contribute to the presence of such fading in the transmission channel.

- *Multipath and Delay Spread:* it describes the dispersive nature of the channel. Usually, there is no LOS path between transmitter and receiver and hence the incoming signal is received from different directions and with different delays. This multipath propagation results in signal smearing or spreading in time. The spreading out effect of the multipath propagation is called delay this delay spread in the received signal leads to inter symbol interference, consequently limiting the maximum data rate supported by the multipath channel. Another characteristic measure of a multipath channel that is closely related to delay spread is the coherence bandwidth B_c. Coherence bandwidth represents the range of frequencies over which the channel's response is considered flat (spectral components have equal gain and linear phase). Consequently, frequency components that are separated by more than the coherence bandwidth will be affected differently by the channel [21][23].

- *Doppler Spread:* it describes the time varying nature of the channel. As the receiver is moving with respect to the transmitter, the received

signal will have different frequency from that of the source due to Doppler Effect. For instance, if a single tone signal of frequency f_1 is transmitted, the received signal's spectrum or the Doppler spectrum will have components in the range ($f_1 \pm f_d$), where $f_d = \frac{v}{\lambda}$. The effect of spectral spreading is called the Doppler spread. Furthermore, a dual parameter to the Doppler spread is called the coherence time. The coherence time T_c is defined as the time duration over which the channel impulse response is essentially constant and is estimated using the maximum Doppler spread of the channel.

According to the relationship between the channel parameters, such as delay spread and coherence bandwidth, and signal parameters (symbol rate and bandwidth), the signal may undergo different types of fading. For example, multipath delay spread causes dispersion of signal in time and leads to frequency selective fading of the channel. On the other hand, Doppler spread leads to frequency dispersion and time selective fading of the channel. The different types of channel fading are summarized in Figure 2.1 depending on the signal as well as channel parameters [23].

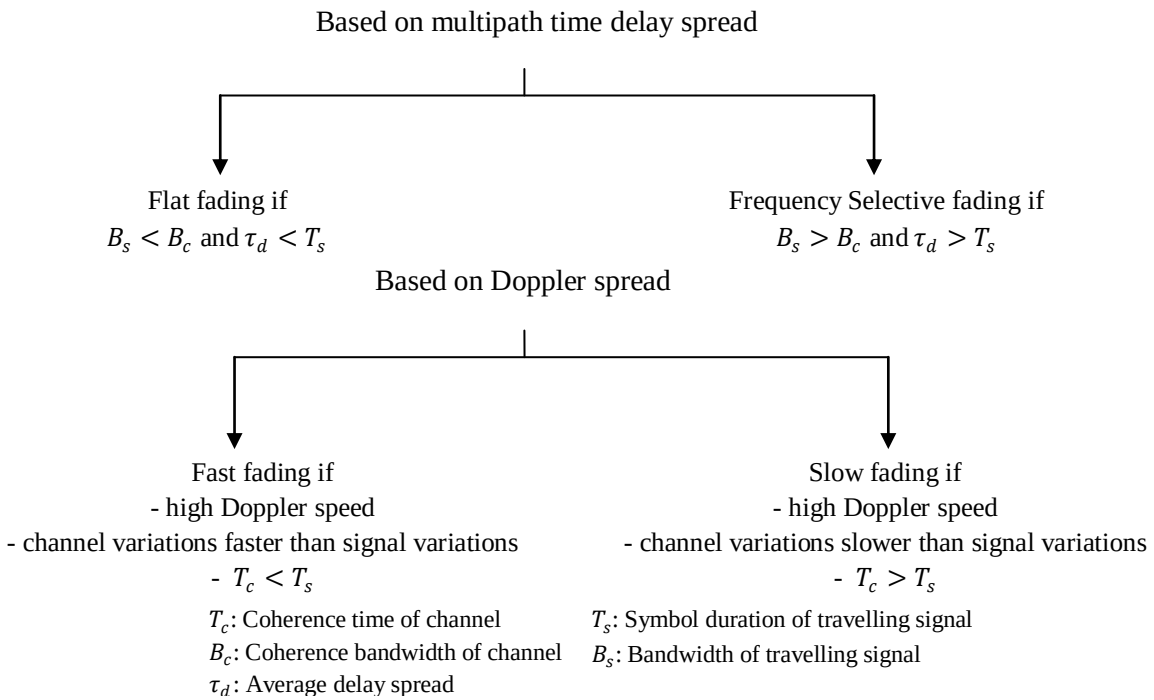

Figure 2.1. Small Scale fading classification based on multipath delay spread and Doppler spread.

2.3 Pattern Recognition

As will be discussed later in this thesis, spectrum sensing in CR networks can be thought of as a pattern recognition problem. Generally speaking, pattern recognition examines tools to classify a given set of data into several different categories. Typical problems addressed by pattern recognition include speech recognition and face recognition where an image is categorized 'person's face' or 'not'. Pattern recognition was utilized mainly in signal classification rather than spectrum sensing. For instance, various pattern recognition techniques were utilized to classify an incoming received signal into different modulation types [24][25].

2.3.1 General Overview of Pattern Recognition

Pattern recognition is a very broad area that has various applications in different fields including engineering and science. As humans, we develop different recognition capabilities including recognizing faces, understanding spoken words, reading handwriting, and distinguishing fresh food from its smell and so on. In pattern recognition systems, these recognition capabilities are given to machines in order to recognize different features from given signals and match them to a known set of classes. Hence, the main aim of pattern recognition is assigning a signal to one of a number of known categories based on features derived to emphasize commonalities between those signals. A generic term that is used to describe signals that need to be classified in a recognition system is patterns. Usually, the patterns may not be useful for classification process, and hence they need to be processed in order to acquire more useful input to the process [26][27]. This processed information is called *features*, and the process involving acquiring them is called *feature extraction*. The various stages followed for the design of a classification system are shown in Figure 2.2, and are described as follows:

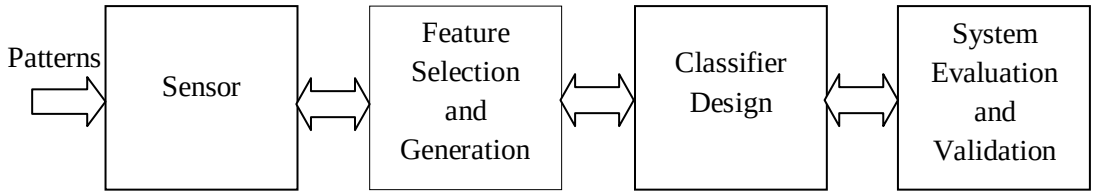

Figure 2.2. Basic stages involved in the design of a pattern recognition system.

- ***Sensing****:* input patterns to the system are acquired using a suitable sensing technique; usually a transducer is used to capture the data, like a camera for images, microphone for voice, and antenna for RF signals. Transducer sensing characteristics such as bandwidth, resolution, sensitivity and distortion may affect the performance of the system.
- ***Feature selection and generation****:* A feature represents the set of data that are useful in classification and discrimination between different outputs. While using raw received signals directly may be a bad choice for classification, a function of the signals may carry discriminative features that are easier to classify. Feature extraction stage may reduce the dimensionality of the received patterns without losing useful information, by discarding redundant data. In other words, feature selection can be considered as a transformation (linear or nonlinear) of incoming data in order to generate class representative feature vectors.
- ***Classifier design****:* when designing a classifier, an important stage is to select the statistical model that fits the statistics of the extracted features. Different parameters are taken into consideration when designing a classifier, such as the dimensionality of the feature space (number of input features) and the nature of the decision boundaries in the feature space (linear or non-linear). For instance, low dimensionality of feature space may not be sufficient for classification; yet, very large feature space can lead to a very slow training, without adding to system's performance.
  - One of the issues to be considered when designing a classifier is to avoid model over-fitting [28]. Over-fitting occurs when the designed model adjusts very much to the training data such that it cannot generalize to other testing data. In other words, the classification loses its capability to classify unknown data based on what it has learnt from the training set.

Usually, this problem arises when complex models are chosen for classification, since they have large parameter space. Hence, it becomes easy for the model to find a parameter combination that fits the training data perfectly; yet fails to generalize to other unseen input data.

- ***System evaluation and validation*:** the final stage is to evaluate the performance of the designed classifier based on classification error rate.

It is important to note that the design stages in Figure 2.2 are not independent; however, they are interrelated. Therefore, depending on the results, we may redesign earlier stages in order to improve the overall performance of the recognition system.

Pattern recognition models can be classified into two classes based on the availability of training data, used in classifier modeling. In some models, a set of training is available and the classifier is designed by exploiting this a priori known information. Once the model parameters are estimated, the model can be used to classify new unknown data. Alternatively, training data set, of known class labels, may not be available for classifier design. In this type of problem, the classifier is given a set of features and it is required to unravel the underlying similarities and cluster similar vectors together. The former way of training is known as supervised pattern recognition, while the latter is called unsupervised pattern recognition or clustering [26].

2.3.2 Pattern Recognition Models

In this section, two of the supervised pattern recognition models, namely artificial neural networks and polynomial classifiers, are described.

2.3.2.1. Artificial Neural Networks (ANN)

2.3.2.1.1. Definition

Artificial neural network (ANN) model was first developed by McCulloch and Pittes in the 1940's as a system for logic computations. ANNs are information processing paradigms that emulate the behavior of the biological neural system in learning attitude. The human brain consists of millions of neurons that transmit signals to and from the brain at a speed of around 200mph [27]. These neurons are interconnected in very complicated

networks that provide intercommunication path for the signal from the brain to other neurons, muscle cells, glands etc. In a similar fashion, ANNs are composed of layers built from large number of interconnected processing elements working in union to solve a specific problem. Each processing element receives connections from other processing elements and/or from itself. The signals flowing on the connections are scaled by adjustable parameters called weights. The sum of the scaled processing input elements is used to obtain intermediate hidden processing elements that contribute to the ANN final output. ANNs are like the human brains, learn by examples and hence they are configured for a specific application, such as pattern recognition, through learning process.

2.3.2.1.2. Neuron Model

A neuron is the basic building block of a neural network, which is shown in Figure 2.3. A neuron consists of the following elements: a sequence of input data $x = [x_0, x_1, x_2, \dots, x_N]$ and the weights, w_i for $i = 0 \dots N$, that connect the input to the neuron. Conventionally, $x_0 = 1$ and its corresponding weight is called the bias. Hence, the neuron consists of N independent inputs and a bias weight that is added to the scaled input summation. In order to transform the summation into an output, an activation function $f(.)$ is applied to the input summation as follows:

$$y = f[(\sum_{i=1}^{N} x_i w_i) + w_0] \qquad (2.3)$$

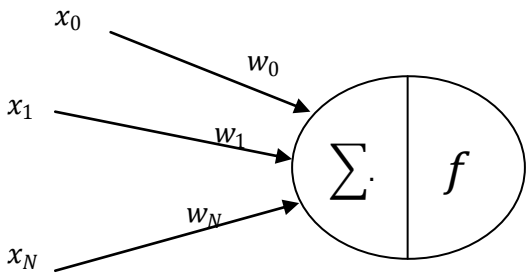

Figure 2.3. A neuron: a fundamental building block of a neural network.

Equation (2.3) justifies the bias term w_0 as an additive constant that moves the sum to the input region of the activation function. The activation function can be linear or non-linear and its type characterizes the neural network. Different activation/transfer functions are used for different applications. The three mostly used functions are:

- Unit step function
- Linear transfer function, which is utilized when the classes are linearly separable.
- Sigmoid transfer function, which is usually used to capture the nonlinearities in the decision boundaries.

It should be noted that ANN follows a non-parametric training, where the weights are adjusted directly from the training data without any assumptions about the statistical distributions of the data. In other words, ANN models utilize training algorithms to modify the weights such that an accurate classification is achieved.

2.3.2.1.3. Network structure

Arbitrary networks of neurons can be very complex; therefore it is desirable to control their complexity and limit their structure. Neurons are thus grouped together to from layers. Each layer has multiple inputs and multiple outputs as shown in Figure 2.4. All inputs to one layer are connected to all its neurons with different weight coefficients. Additionally, all neurons forming one layer will have the same activation function and they are also connected to the neurons in the previous and next layers through a set of weights. The first layer in the network represents the input and last layer is the output at which the number of neurons is equal to the target data dimension. Layers connecting input and output layers are called hidden layers.

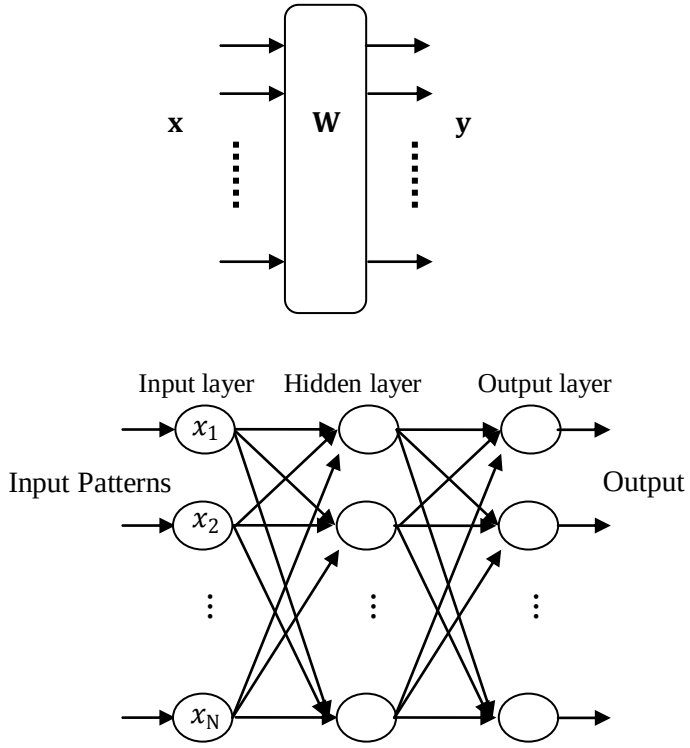

Figure 2.4. a) A multiple- input-multiple output layer of neurons b)A neural network consisting of two layers of neurons.

Starting with a single layer network model with N neurons, presented in Figure 2.4a, we can define the following layer parameters:

$$\mathbf{x} = [x_1, x_2, x_3, \dots, x_N]^T \tag{2.4}$$

$$\mathbf{W} = [\mathbf{w}_1, \mathbf{w}_2, \mathbf{w}_3, \dots, \mathbf{w}_k] \tag{2.5}$$

$$\mathbf{y} = [y_1, y_2, y_3, \dots, y_k]^T \tag{2.6}$$

where $\mathbf{x}, \mathbf{W}, \mathbf{y}$ are the inputs, weights, and outputs for a single layer, respectively. $x_i, w_i, and\ y_i$ are the single input, weight and output for a single layer respectively, T is the transpose of a matrix, N is the number of input features and k is the number of neurons in a layer. Hence, the layer output can be represented by:

$$\boldsymbol{y} = f(\mathbf{wx}) \tag{2.7}$$

This single layer modeling can be extended to a complete network by cascading layers that are interconnected through a set of weights. If the network has C layers, then each layer can be described by an input x^c, a weight matrix w^c, an output y^c and activation function $f(.)^c$, such that the input to each hidden layer is the output of the previous layer $x^c = y^{c-1}$.

2.3.2.2. Polynomial Classifier (PC)

In this section, a special case of neural networks, namely polynomial classifiers (PCs), which represents the essence of this research, is discussed in details. A description of the basic classifier structure is given, followed by the classifier modeling algorithm [29][30][31].

2.3.2.2.1. Classifier's Structure

Polynomial classifier can be considered as a single-hidden layer neural network that not only uses the features of the input pattern as input to the recognition system, but also uses polynomial terms of the input. Polynomial classifiers have been introduced in [32] and have shown several advantages over other recognitions methods (e.g. neural network, hidden Markov models, etc) in speech and speaker recognition applications. These advantages include identification efficiency and better recognition performance. Furthermore, polynomial classifiers deal with simple mathematical operations such as multiplication and summation that fits modern digital signal processing (DSP) circuits and hence result in less computational and storage requirements.

The principle of polynomial classifier is that it expands the input feature space into a higher dimensional space. The basic embodiment of a polynomial classifier can be realized with the block diagram given in Figure 2.5.

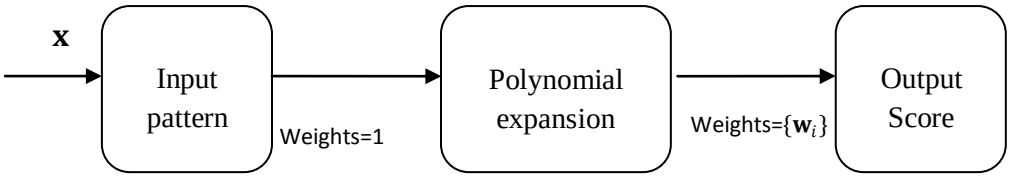

Figure 2.5. Block diagram of a polynomial network.

Consider an input pattern to the network $\mathbf{x} = [x_1, x_2, x_3, \dots, x_N]^T$, where N is the number of features. The input data $\mathbf{x}$ is directly observed by second block with unity weights that are not changed during the estimation process. The second block consists of the vectorial mapping form the N- dimensional feature vector, $\mathbf{x}$ into an l-dimensional vector $\boldsymbol{\varphi}(\mathbf{x})$. The elements of $\boldsymbol{\varphi}(\mathbf{x})$ are monomials of the form [31]:

$$\boldsymbol{\varphi}(\mathbf{x}) = [\,1 \;\; x_1 \;\; x_2 \;\; x_3 \;\; x_4 \dots x_N \;\; {x_1}^2 \;\; x_1x_2 \;\; x_1x_3 \;\; \dots \;\; {x_1}^3 \;\; {x_1}^2x_2 \dots]^T \qquad (2.8)$$

Finally, the output score f_k is obtained at the output block after linearly combining the expansion terms $\boldsymbol{\varphi}(\mathbf{x})$.

$$f_i = \mathbf{w}_i^T \boldsymbol{\varphi}(\mathbf{x}) \qquad (2.9)$$

where $\mathbf{w_i}$ is the model of class i. For example, for second order polynomial expansion, $\boldsymbol{\varphi}(\mathbf{x})$ will consist of the second order polynomial terms in (2.8) and f_i becomes:

$$f_i = \left(\sum_{m=1}^{N} w_m x_{m+} \sum_{j=1}^{N} \sum_{m=1}^{N} w_{mj} \; x_m x_j + w_o \right) \qquad (2.10)$$

The dimensionality of the expanded vector $\boldsymbol{\varphi}(\mathbf{x})$ can be expressed in terms of the polynomial order and the dimensionality of the input vector $\mathbf{x}$. Table 2.1 shows the polynomial expansion length for different polynomial expansion orders [29].

Table 2.1. Length of polynomial expansion.

Order	Polynomial Expansion Length
1st	$l_{p1} = N + 1$
2nd	$l_{p2} = l_{p1} + \sum_{i=1}^{N} i$
3rd	$l_{p3} = l_{p2} + N^2 + \frac{N!}{3!\,(N-3)!}$
4th	$l_{p4} = l_{p3} + N^2 + 2\frac{N!}{2!\,(N-2)!} + 3\frac{N!}{3!\,(N-3)!} + \frac{N!}{4!\,(N-4)!}$

2.3.2.2.2. Classifier's Modeling Algorithm

Consider a multiclass classification problem for which the classifier is required to differentiate between N_{classes} possible classes within a multidimensional observation sequence, $\mathbf{X}$ such that [29][30]:

$$\mathbf{X} = \left[\mathbf{x_1}\ \mathbf{x_2}\ \ldots\ \mathbf{x}_Q\right]^T \tag{2.11}$$

and

$$\mathbf{x_i} = [x_{i1}, x_{i2}, x_{i3}, \ldots, x_{iN}]^T \tag{2.12}$$

where $\mathbf{x_i}$ is an N dimentional feature vector, matrix $\mathbf{X}$ is a sequence of Q N-dimensional feature vectors available for classification, $Q = \sum_{i=1}^{N_{\text{classes}}} q_i$ represents the total count of feature vectors in the training data set, and q_i is the number of feature vectors belonging to class i. Our goal is to solve for the best model parameters $\{\mathbf{w}_i\}$ that minimizes the Euclidian distance between $f_i(\mathbf{X})$ in (2.9) and the desired ideal output $\{\mathbf{t}_i\}$ for class i . The ideal output $\mathbf{t}_i$ is a column vector of length Q consisting of elements equal to ones for the indices corresponding to class i and zeros otherwise. When the input $\mathbf{X}$ is

applied to the classifier, its columns, representing feature vectors, will be expanded by $\boldsymbol{\varphi}(\mathbf{X})$ as in (2.8) resulting in a model training data set $\mathbf{M}$ of size $(Q \times l)$ that is defined by:

$$\mathbf{M} = [\boldsymbol{\varphi}(\mathbf{x}_1) \quad \boldsymbol{\varphi}(\mathbf{x}_2) \dots \boldsymbol{\varphi}(\mathbf{x}_Q)]^T \tag{2.13}$$

Once training feature vectors are expanded into their polynomial basis terms, the classifier needs to be trained to match the output target $\mathbf{t}_i$ for class i. Hence the resulting problem using mean-squared error criterion can be formulated as:

$$\mathbf{w}_i^{\text{opt}} = \underset{\mathbf{w}}{\text{argmin}} \|\mathbf{M}\mathbf{w} - \mathbf{t}_i\|_2 \tag{2.14}$$

The problem of (2.13) can be solved using the method of normal equation [32] [33]:

$$\mathbf{M}^T\mathbf{M}\mathbf{w}_i^{\text{opt}} = \mathbf{M}^T\mathbf{t}_i \tag{2.15}$$

which is used to compute class models $\{\mathbf{w}_i\}, i = 1,2 \dots, N_{\text{classes}}$. After training, the estimated class models $\{\mathbf{w}_i\}$ are used for classification of novel data sets.

CHAPTER 3

PROBLEM FORMULATION AND METHODOLOGY

In this chapter, we formulate the problem of spectrum sensing in CR networks. The network structure, in which the spectrum sensing problem is formed, is discussed and illustrated. Following that is a definition of the main performance metrics that need to be optimized by the proposed methodology. Later in the chapter, we propose a cooperative approach for spectrum sensing in CR networks with soft decision rule. In the proposed system, more reliable secondary users are given higher weight in making the decision about spectrum vacancy. Specifically, we propose to utilize classification capability of pattern recognition models, discussed in Chapter 2, to identify the available spectrum bands for unlicensed users. A detailed description of the proposed classification scheme as applied to the problem of spectrum sensing is explained.

3.1 Network Structure

We consider dynamic resource allocation in a multiple secondary user CR network with the structure illustrated in Figure 3.1. The CR network consists of N cognitive users with a central node (e.g. base station) that detects the presence of primary signals, decides on the channel availability, and allocates the available bands to CRs. Primary users' network and CR network are assumed to coexist within the same geographical area. CRs temporarily access the under-utilized licensed frequency bands, without harmful conflict with primary spectrum holders' usage.

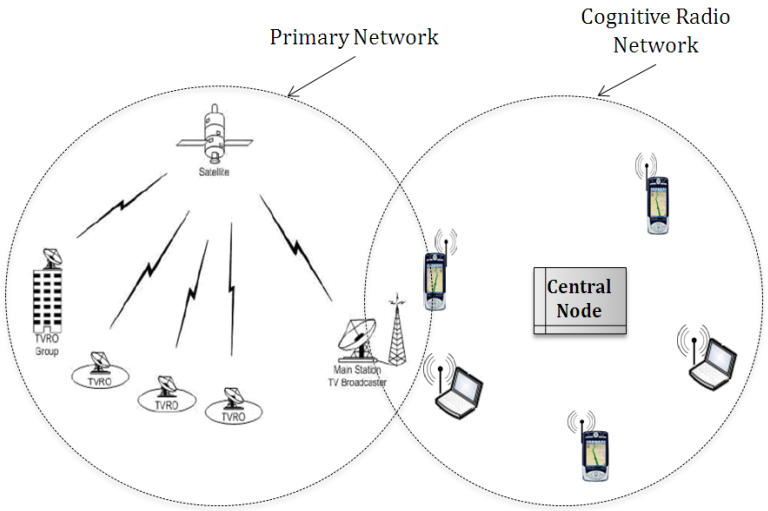

Figure 3.1. Illustration of centralized CR network coexisting within primary network's geographical area.

The above scenario can be envisioned in applications, where heavy spectrum demands often take place in unlicensed bands while licensed bands experience low or medium utilization [33]. Such primary applications include TV broadcasting and cellular systems' bands in rural areas where there is a little demand on cellular communications. For example, IEEE 802.22 standard proposes reusing inactive TV channels without causing interference to the incumbent TV receivers. The unused spectrum can be utilized by WLAN users to efficiently increase their data rates [2].

In the proposed system, secondary users are constantly sensing the target spectrum band for primary signal presence. Within a secondary user receiver, discriminative features are extracted from the observed signal in order to detect inactivity of primary users' network. The extracted features are transmitted to the CR base station through a relatively low data rate control channel. The network control channel is allocated for exchanging network information between CRs and CR base station, in addition to broadcasting channel allocation information to CRs. Decision is made by CR base station based on a pattern recognition classifier that is adequately trained to detect the activation of target frequency bands.

When dual-radio architecture is deployed, CRs monitor the target spectrum in a given area while simultaneously transmitting data. Alternatively, secondary users observe the spectrum for a given sensing time, wait for the global decision made by CR base station, and then start transmission. The latter sensing algorithm is applied

when single-radio architecture is implemented. In this research, CRs are assumed to implement dual-radio architecture, where a separate radio chain is employed for spectrum monitoring, feature transmission, and channel allocation. The CR network sensing algorithm can be deployed as illustrated in Figure 3.2.

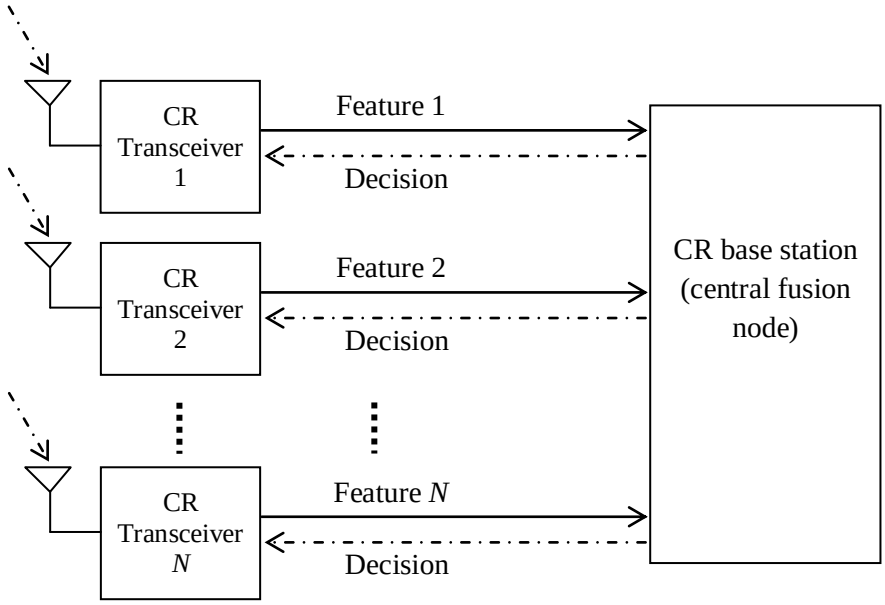

Figure 3.2. Block diagram of CR monitoring spectrum and communicating with centralized CR base station.

3.2 Performance Metrics

In this section, we introduce the metrics used to evaluate the performance of the resource sharing system in a CR network, in addition to its impact on the primary users' network. These metrics include level of interference to primary users and spectral utilization efficiency. We identify two quantities that are closely related to interference level and spectral utilization efficiency, namely detection probability (P_d) and false alarm probability(P_f). Detection probability refers to the probability that a CR correctly decides the target spectrum is busy, when primary transmission is taking place. If primary transmission is correctly detected by CR users, the target spectrum will not be utilized by the CR network. Hence, a high detection probability corresponds to a low level of interference with primary users when the spectrum is occupied. False alarm probability; on the other hand, is the probability that the CR makes a wrong decision that the spectrum is occupied while it is actually not. Having a high false alarm probability lowers the spectral utilization, since spectral opportunities are missed due to falsely detecting primary transmissions. The

requirements of maximum detection probability and minimum false alarm are highly desirable, but contradicting. Hence, our aim is to design a spectrum sensing algorithm that maximizes detection probability, while keeping the false alarm below a given design constraint. The two performance metrics, mentioned above, will be used to evaluate the performance of the proposed system.

3.3 System Model

In this research, we utilize supervised pattern recognition techniques (explained in section 2.3) at the CR base station as a mean to classify available spectrum holes, such that maximum detection is achieved with a desired false alarm rate. Collaborative secondary users monitor the spectrum and then provide discriminative features to the CR base station. In supervised learning, a training data sequence is available and the classifier is designed by exploiting this sequence. Once the model parameters are estimated, the model is used to classify novel data.

The CR base station applies the received features from different users to a trained classifier, where a decision is made about the existence of primary transmission. The general stages of pattern recognition system design, depicted in Figure 3.3, are discussed as follows:

3.3.1 Sensing

CRs perform spectrum sensing of the received signal at a rate of f_s samples/second. The binary hypothesis test for spectrum sensing is formulated as follows:

$$x_j[n] = \begin{cases} g_j\ s\ [n] + n_j[n] : & H_1 \\ n_j[n] : & H_0 \end{cases} \quad \text{for } j = 1,2, \dots N \quad (3.1)$$

where $x_j[n]$ represents the received signal by the j^{th} user at the n^{th} instant of time, and $s\ [n]$ denotes the primary signal. Further, H_1 represents received hypothesis of an occupied spectrum, while H_0 corresponds to an idle spectrum. The received signal at the j^{th} user is corrupted by a zero-mean additive white Gaussian noise (AWGN), $n_j[n]$ with variance σ^2. The primary signal passes through a wireless channel with channel gain equivalent to g_j. The channel is modeled as a flat channel with slow

fading. Each cognitive user receives a single path with channel coefficient whose magnitude is Rayleigh distributed and its phase is uniformly distributed in $[0,2\pi)$. Additionally, different CRs in the network are assumed to have independent and identically distributed (i.i.d.) channel coefficients. Since a slow fading channel is considered, the channel coefficients are assumed to be constant over a number of received signal symbols. Therefore, the coherence time of the channel, T_c is set to be much larger than primary signal's symbol duration.

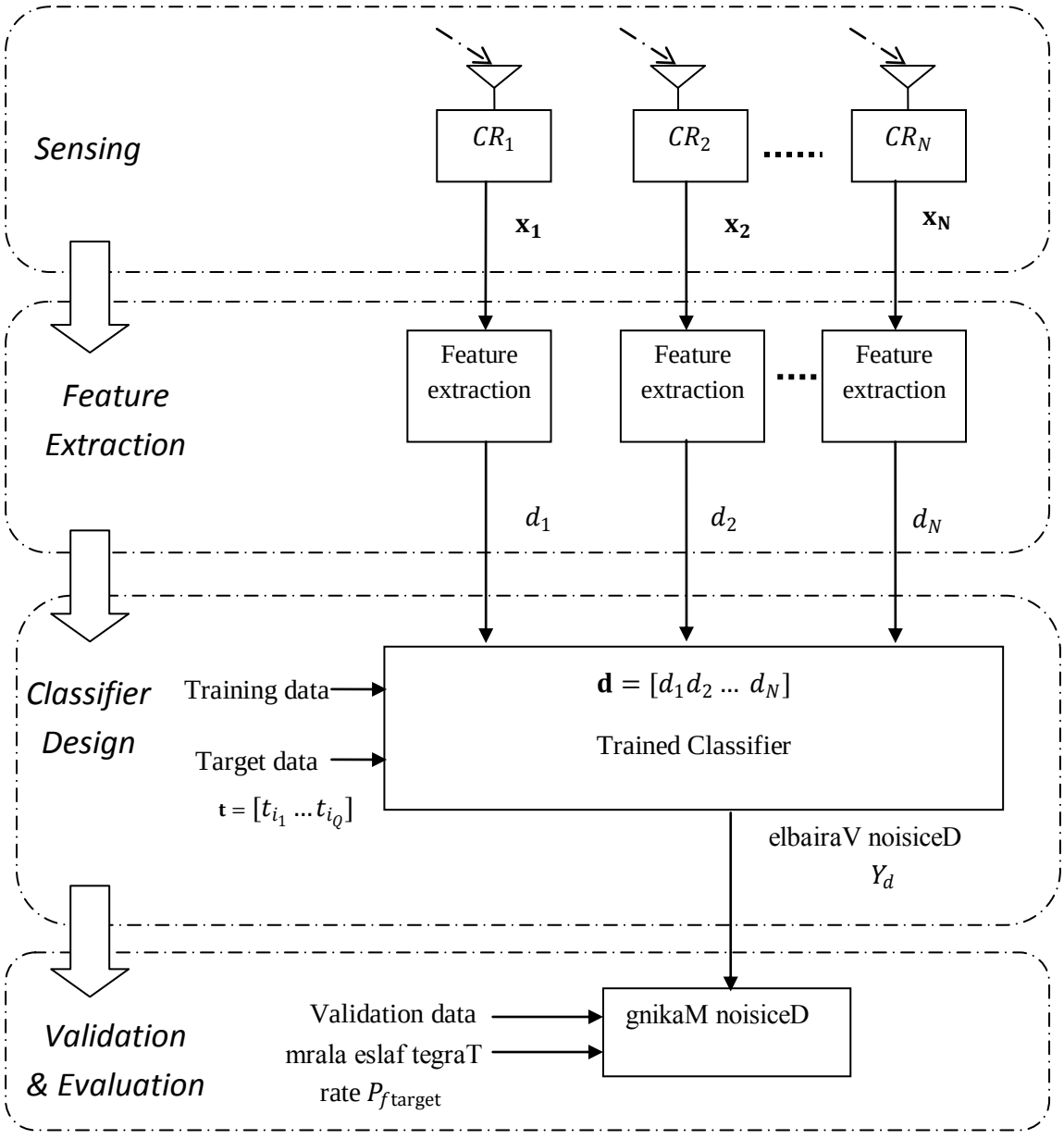

Figure 3.3. Proposed CR system model for spectrum sensing.

3.3.2 Feature Extraction

At each CR, the received signal is applied to the feature extraction block, where a local decision variable d_j is computed based on a fixed window. Size of the chosen window corresponds to M samples or equivalently a sensing time interval of $\Delta t = MT_s$, where $T_s = 1/f_s$. The local decision variable is computed based on the type of information available at the secondary user. Consequently, spectrum sensing is classified into non-parametric or parametric spectrum sensing based on the prior knowledge of the primary signal.

In non-parametric spectrum sensing, secondary users in a CR network have no prior information about the transmitted primary signal. The feature extraction stage will include schemes like energy and autocorrelation based detection. Energy detection algorithm involves utilizing the energy of the received signal at the classifier to discriminate between noise only and primary signal. However, in autocorrelation detection, the differences in the autocorrelation characteristics between the noise and licensed users' signals are utilized to identify the vacant spectrum by the classifier. Alternatively, in parametric sensing, prior information including carrier frequency and synchronizing patterns are assumed to be known about the primary user's signal. In this case, feature extraction will be achieved by either exploiting cyclic features present in the signal or through coherent detection.

Features extracted by any of the above detection schemes will follow a certain pattern when the spectrum is occupied by a primary user. The pattern extracted would be different when only noise is present in the spectrum. The difference between these two patterns will be exploited as discriminative input data to the classifier for decision making.

3.3.3 Classifier Design

The classifier model to be implemented for spectrum sensing in CR network is the polynomial classifier discussed in section 2.3.2. The problem of spectrum sensing can be formulated as a multi-input single-output (MISO) polynomial classifier. Features extracted by different receivers, $\mathbf{d} = [d_1 \ldots d_N]$, form an N-dimensional input vector to the classifier. The classifier is required to provide a single output score Y_d, representing the decision of whether or not a primary signal is present.

The classifier model design comprises of two stages:

- Model Training

The training process involves finding the optimal model parameters that best map a multidimensional input sequence to a corresponding one dimensional target sequence. The model is designed to classify between two different classes, H_i for $i = \{0,1\}$, corresponding to the binary hypothesis in (3.1). The multidimensional input sequence $\mathbf{D}_{\text{train}}$ is a $Q \times N$ matrix, where N is the dimensionality of the input feature vectors (provided by N CR users) and Q is the number of feature vectors used in the training process. The training matrix $\mathbf{D}_{\text{train}}$ is given by:

$$\mathbf{D}_{\text{train}} = \begin{bmatrix} d_{1,1}\, d_{1,2} & \cdots & d_{1,N} \\ \vdots & \ddots & \vdots \\ d_{Q,1}\, d_{Q,2} & \cdots & d_{Q,N} \end{bmatrix} \tag{3.2}$$

The one dimensional target vector $\mathbf{t_i}$ is given by:

$$\mathbf{t_i} = \begin{bmatrix} t_{i_1} \\ \vdots \\ t_{i_Q} \end{bmatrix} \tag{3.3}$$

and consists of Q elements where:

- $t_{i_z} = 1$, for $z = 1,2 \ldots Q$, if the corresponding z^{th} feature vector belongs to class i.
- $t_{i_z} = 0$, for $z = 1,2 \ldots Q$, if the corresponding z^{th} feature vector does not belongs to class i.

The training vectors in $\mathbf{D}_{\text{train}}$ are expanded into their polynomial terms defined in (2.8), resulting in a training matrix $\mathbf{M}$ of size$(Q \times l)$, where Q is the number of training feature vectors and l is the number of expansion terms. Thereafter, the polynomial classifier is trained to find an optimum set of weights, $\mathbf{w}$ that minimizes the Euclidian distance between the ideal target vector $\mathbf{t_i}$ and the training matrix $\mathbf{M}$ using mean-squared error as objective criterion, by solving the problem in (2.14). As a

reminder, the optimal model weights if solved such that it satisfies $\mathbf{w_i^{opt}} = \underset{\mathbf{w}}{\operatorname{argmin}} \|\mathbf{Mw} - \mathbf{t_i}\|_2$.

The optimum model weights are obtained explicitly by applying the normal equations method in (2.15), which can be modified for the two classes case considered in spectrum sensing:

$$\begin{aligned} \mathbf{M}^T\mathbf{M}\mathbf{w}_1^{\text{opt}} &= \mathbf{M}^T\mathbf{t_1} \quad : H_1 \\ \mathbf{M}^T\mathbf{M}\mathbf{w}_0^{\text{opt}} &= \mathbf{M}^T\mathbf{t_0} \quad : H_0 \end{aligned} \tag{3.4}$$

A block diagram illustrating the training stage in the polynomial classifier is presented in Figure 3.4.

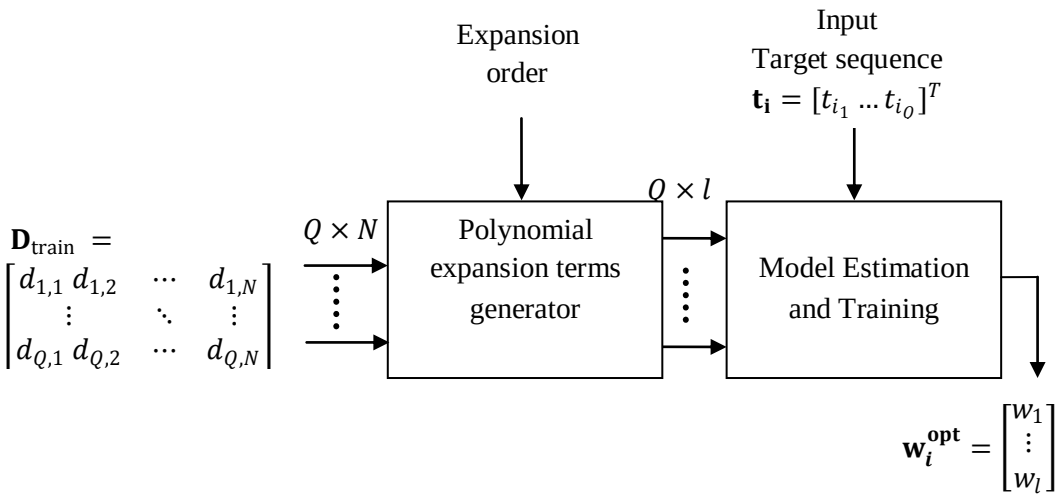

Figure 3.4. Block diagram of classifier training stage.

- Model testing

In the testing stage, novel feature vectors $\mathbf{d}_{\text{test}}$ are used to represent the testing data set. The features are initially expanded into their basis terms $\boldsymbol{\varphi}(\mathbf{d}_{\text{test}})$ and then presented to the trained models $\{\mathbf{w}_0^{\text{opt}}, \mathbf{w}_1^{\text{opt}}\}$ to obtain the corresponding set of scores y_i.

$$\{y_i\} = \boldsymbol{\varphi}(\boldsymbol{x})\, \mathbf{w}_{\text{i}}^{\text{opt}} \qquad \text{for } i = 0,1 \tag{3.5}$$

Accordingly, we assign the testing feature vector to hypothesis H_i that satisfies (3.6) [29]:

$$Y_d = \underset{i}{\operatorname{argmax}}\{y_i\} \tag{3.6}$$

The block diagram for the model testing of polynomial classifier is depicted in Figure 3.5.

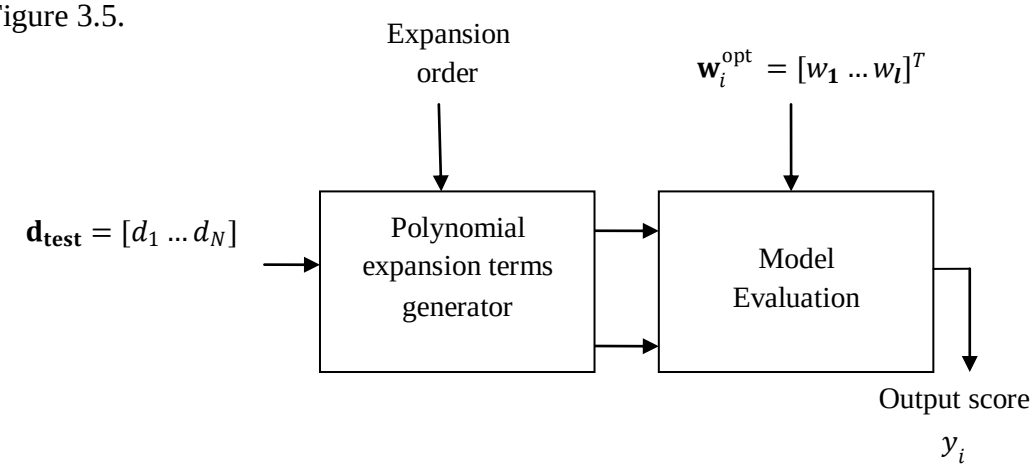

Figure 3.5. Block diagram of classifier testing stage.

3.3.4 Validation and Evaluation

Ideally, the classifier model $\mathbf{w}_1^{\text{opt}}$ is expected to output a score of one when spectrum is occupied and zero when spectrum is idle. Similarly, an output score of one is expected when spectrum is idle and zero when spectrum is occupied on testing the classifier model $\mathbf{w}_0^{\text{opt}}$. However, when testing data are fed to the classifier, scores varying around one and zero are obtained. By comparing the output score obtained from both models, a decision is made about the input feature vector, that it belongs to the class with maximum output score as in (3.6).

However, in order to achieve a desired level of constant false alarm rate, a threshold needs to be defined to separate the two classes instead of just comparing different models' output scores. The threshold setting is done during the validation stage, as a post-processing operation in order to obtain meaningful output at the classifier.

For this purpose, a validation data sequence $\mathbf{D}_{\text{valid}}$, similar to the training sequence, is used. The validation data consists of Q N-dimensional feature vectors. The ideal outputs $\mathbf{t}_1$ for the model $\mathbf{w}_1^{\text{opt}}$, corresponding to validation feature vectors are known (i.e. zeros for empty spectrum and ones for an occupied spectrum). First, the following algorithm was followed:

- Validation data are subjected to the classifier model $\mathbf{w}_1^{\text{opt}}$.

- Since classifier is designed to give an output y_1 altering between 1 and 0, the threshold is initialized to $\lambda = 0.5$. Hence, the global decision variable $Y_d = 1$ if $y_1 > \lambda$ and vice versa.
- The resultant false alarm rate is then estimated, by comparing the output decisions of all validation feature vectors to the ideal output $\mathbf{t}_1$. The ratio between the number of times the classifier falsely decides the spectrum is available $(Y_{d_z} = 1)$, to the total number of times the spectrum is actually available represents the false alarm probability$(t_{1_z} = 0)$.

The above algorithm was found to result in a varying false alarm rate that is not controlled, especially with different input signal to-noise ratio. Hence, an iterative algorithm is applied to set a threshold for different SNR levels that achieves a specific false alarm rate. The algorithm is implemented as follows:

- The output score is computed, by subjecting validation data to the model $\mathbf{w}_1^{\text{opt}}$.
- The threshold is initialized to $\lambda = 0.5$, such that the global decision variable $Y_d = 1$ if $y_1 > \lambda$ and vice versa.
- The resultant false alarm rate is then estimated, by comparing the output decisions of all validation feature vectors to the ideal output $\mathbf{t}_1$.
- The threshold λ is incremented or decremented such that the desired false alarm rate is achieved with a mean-squared error of 1%.
- The above steps are repeated for many validation data with different received SNR levels.

Note that the above threshold setting operation, in addition to the training process is performed offline. The training and validation data sequences are retrieved from a database that is maintained at the CR base station for offline training and validation. Finally, the trained classifier models and the pre-calculated thresholds are later used to separate output classes for novel input data to the classifier.

CHAPTER 4

NONPARAMETRIC SPECTRUM SENSING

In this chapter, the proposed classification and recognition system is applied to cooperative CR networks to detect the ongoing primary transmission, when secondary users have limited information on the primary signal. In nonparametric sensing, we propose to identify the presence of primary signal based on energy and autocorrelation features. In this chapter, the nonparametric sensing schemes, are first described and analyzed. Thereafter, simulation results representing the performance of each of the nonparametric sensing schemes are presented, when applied to the proposed classification system. Further, a comparison between the two nonparametric schemes is illustrated. Finally, concluding remarks are presented.

4.1 Energy Based Feature Extraction

Energy detection is one of the most commonly used techniques in spectrum sensing as it is characterized with low computational and implementation complexity. It is a nonparametric sensing scheme, as it does not require any prior knowledge of the primary users' signal as opposed to other sensing techniques. In this section, the modeled classification system identifies spectrum holes relying on the energy content of the received signal. However, the task of detecting the signal becomes very challenging as the incoming signal level is very low compared noise level [8][14]. The proposed cooperative sensing and classification algorithm facilitates detection with small received signal levels. A block diagram of energy detection is depicted in Figure 4.1.

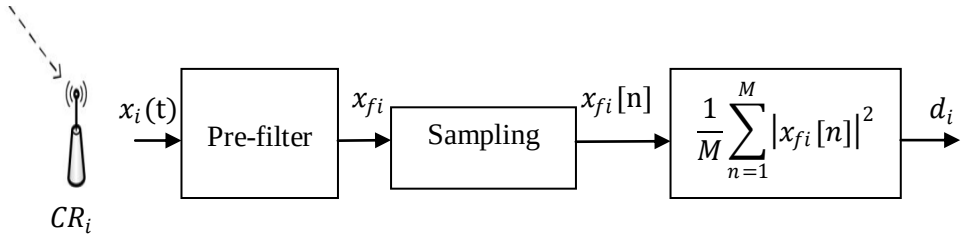

Figure 4.1. Block diagram of energy based feature extraction.

Considering the binary hypothesis defined in (3.1), the received signal $x_i(t)$ by the i^{th} secondary user is pre-filtered for the desired frequency band. The local decision variable, corresponding to extracted feature by the i^{th} secondary user to the classifier model, is hence defined by:

$$d_i = \frac{1}{M}\sum_{n=1}^{M}\left|x_{fi}[n]\right|^2 \tag{4.1}$$

where M is the number of received signal samples during one observation period. For a fixed channel gain, the received signal samples can be modeled as independent and identically distributed (i.i.d.) Gaussian random variables with variance ${\sigma_x}^2$. When the primary signal is absent, the decision variable d_i will be the sum of the square of M Gaussian random variables with zero mean. Hence the decision variable will have a central Chi-square distribution with M degrees of freedom. Whereas, when the primary signal is present the decision variable will have a non-central Chi-square distribution with M degrees of freedom [7]. If the number M is large enough, the central limit theorem can apply and the decision variable is approximated by a non-zero mean Gaussian random variable. Therefore, the local decision variable d_i will have different statistical distributions for different hypothesis representing distinct features for signal identification.

An alternative scheme to realize energy detection is by using the fast Fourier Transform (FFT) computation of the received signal as shown in Figure 4.2 [6] . In this approach, the received signal is sampled in a time window and passed through an FFT device to compute the spectrum $X[k]$. The signal energy is then computed in frequency domain to produce a local decision variable d_i.

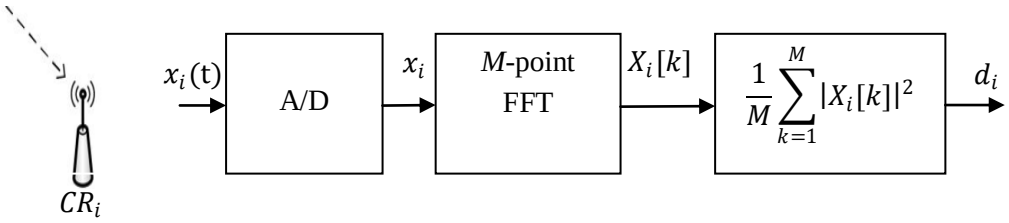

Figure 4.2. Block diagram of energy based feature extraction using FFT computations.

4.2 Autocorrelation Based Feature Extraction

Correlation techniques are utilized in signal detection and hypothesis testing in many fields such as radars and communication systems [1]. Such correlation techniques include spectral correlation in cyclostationary detection, which requires knowledge of primary signal parameters. Moreover, signal detection is performed by exploiting the differences in the envelope of the autocorrelation between existing noise and primary signal. Autocorrelation base detection has been proposed recently as a spectrum sensing technique in CR networks, as an alternative to energy detection [1]. Let us consider the binary hypothesis, defined in (3.1), corresponding to a spectrum sensing scenario, in which a CR makes decision about the availability of the spectrum. Assuming a bandpass linearly modulated primary signal s_{PB}, i.e. phase shift keying (PSK) and pulse amplitude modulation (PAM), it is down converted into its baseband equivalent $s_l(t)$. The baseband equivalent $s_l(t)$, which is a zero mean wide sense stationary process, has the following form:

$$s_l(t) = \sum_n \sqrt{E_s} d_n h(t - nT) \tag{4.2}$$

where E_s is the energy per symbol, transmission rate is $\frac{1}{T}$ symbols/second, $h(t)$ is a real valued signal pulse representing a signal symbol, and $\{d_n\}$ represents the sequence of symbols that results from mapping k- bits into the corresponding signal space diagram. In binary phase shift keying (BPSK), the sequence d_n is real valued and takes a value of ± 1. The autocorrelation function of the received signal by the i^{th} user is given by:

$$R_x(t + \tau, t) = E[x^*(t)x(t + \tau)] \tag{4.3}$$

where $E[.]$ is the expectation operator. Assuming that the primary signal is independent from the envelope of the channel and R_x is estimated for the different hypothesis by (4.4):

$$R_x(t+\tau,t) = \begin{cases} E[|g|^2]R_s(\tau) + R_n(\tau) : & H_1 \\ R_n(\tau) : & H_0 \end{cases} \quad (4.4)$$

where

$$R_s(\tau) = E[s^*(t)s(t+\tau)] = \sum_{n=-\infty}^{\infty}\sum_{m=-\infty}^{\infty} E[d^*{}_m d_n]h(t-nT)h(t+\tau-mT) \quad (4.5)$$

Assuming that the data sequence d_n is a zero mean wide-sense stationary with an autocorrelation

$$R_d(m,n) = E[d^*{}_m d_n] \quad (4.6)$$

and the autocorrelation function of $h(t)$ defined as

$$R_h(\tau) = \int_{-\infty}^{\infty} h(t)h(t+\tau)dt \quad (4.7)$$

Then, (4.5) reduces to [34], pp. 204-206]:

$$R_s(\tau) = \frac{1}{T}\sum_{m=-\infty}^{\infty} R_d(m)\ R_h(\tau - mT) \quad (4.8)$$

The autocorrelation of the pulse signal is an even function of τ , and hence $R_h(\tau - mT) = R_h(mT - \tau)$ [34] [31]. By substituting $R_h(mT-\tau)$ in (4.8), $R_s(\tau)$ can be interpreted as the convolution of R_d with R_h:

$$R_s(\tau) = R_d(m) * R_h(\tau) \quad (4.9)$$

Therefore, the characteristics of the autocorrelation of the primary signal are determined by two factors. The first factor is the shape of the basic pulse used for shaping and the second is the correlation properties of the transmitted data sequence. Moreover, assuming a BPSK primary signal with information symbols $\{d_n\}$ that are uncorrelated zero-mean random variables, each with a unit variance, its autocorrelation function is defined as in (4.10) [34].

$$R_d(m) = \begin{cases} 1 & for\ m = 0 \\ 0 & otherwise \end{cases} \tag{4.10}$$

Substitution of (4.10) into (4.9) yields a convolution of an impulse with the autocorrelation of pulse shaping function, resulting on the autocorrelation function of $h(t)$:

$$R_s(\tau) = \delta(\tau) * R_h(\tau) = R_h(\tau) \tag{4.11}$$

Utilizing the duality between the power spectral density and the autocorrelation of a random process, the AWGN process with power spectral density of $N_0/2$ W/Hz will have an autocorrelation of $R_n = \frac{N_0}{2}\delta(\tau)$. Assuming channel gains are constant during the estimation of autocorrelation, (4.4) can be rewritten as:

$$R_x(t+\tau, t) = \begin{cases} |g|^2 R_h(\tau) + \dfrac{N_0}{2}\delta(\tau) & : \quad H_1 \\ \dfrac{N_0}{2}\delta(\tau) & : \quad H_0 \end{cases} \tag{4.12}$$

Hence, by estimating the autocorrelation of the received signal over an observation window, we can distinguish between the presence and absence of the primary signal. However, due to fading, the primary signal autocorrelation will be scaled by channel gains as in (4.12). For an illustration, let us consider a rectangular pulse shaping function $h(t)$ of width T, it will have a triangular autocorrelation function cantered around a delay $\tau = 0$ of width $2T$, as illustrated in Figure 4.3.

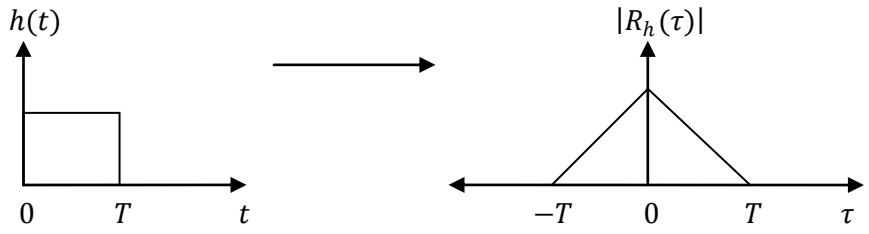

Figure 4.3. Rectangular pulse and its autocorrelation $R_h(\tau)$.

By integrating the estimated autocorrelation of the received signal over the delay interval $\tau \in [-T, T]$, we can obtain a discriminative decision variable d_i between noise only and the primary signal. This is possible, since the autocorrelation of noise is theoretically concentrated around zero, unlike the primary signal's autocorrelation that is distributed within a wider range.

However, (4.12) is only valid when channel gains are constant during the observation window, over which the autocorrelation is calculated. Since the primary signal is assumed to have undergone slow flat fading, the channel gain is constant for a number of symbol durations represented by the channel coherence time T_c. However, if the observation window length exceeds the coherence time of the channel, the channel gain will vary, and hence $E[|g|^2] \neq |g|^2$. Accordingly, we propose dividing observation window into subsections over which the autocorrelation is computed. The subsection duration is chosen such that the channel gains are approximately constant over it.

The estimation of autocorrelation based on subsection-averaging will serve two purposes. The first is to utilize diversity, provided by different subsections of the received signal affected by different channel gains. The second is to reduce the erratic behaviour of received signal's autocorrelation, since the added noise variance is reduced by averaging. To illustrate, assume B independent random variables with the same mean μ and same variance σ^2. The sample mean of these random variables is μ and their variance is equal to σ^2/B. Hence, the effect of noise is inhibited considerably due to subsection averaging.

Autocorrelation based detection is conducted through the following steps:

1) The received signal by the CR is down converted and sampled to obtain $x_i[n]$, in which every M bits are used in producing a local decision variable d_i. The input time series $x_i[n]$ is divided into B subsections, each of C bits-length $x_{ij}[n]$, where $M = BC$.

2) Then, the autocorrelation is estimated for each subsection:

$$R_{xj}[k] = \frac{1}{C}\sum_{n=0}^{C-1} x_{ij}[n]x_{ij}[n-k], \text{for } k = [0, \pm1, \pm2, ..], i = \{1,2 \dots N\} and \ j \in [1, B] \quad (4.13)$$

3) After computing the autocorrelation of different subsections, an average autocorrelation function $R_{\text{avg}}[k]$ is acquired by averaging subsection autocorrelations $R_{xj}[k]$:

$$R_{\text{avg}}[k] = \frac{1}{B}\sum_{j=1}^{B} R_{xj}[k] \tag{4.14}$$

4) The estimated autocorrelation $R_{\text{avg}}[k]$ is then summed over delays $k \in [-N_{\text{sym}}, N_{\text{sym}}]$, for which N_{sym} represent the number of samples in one primary symbol, in order to obtain a local decision variable:

$$d_i = \sum_{k=-N_{\text{sym}}}^{N_{\text{sym}}} R_{\text{avg}}[k] \qquad i = \{1,2 \dots N\} \tag{4.15}$$

4.3 Numerical Results

In this section, first order polynomial classifier, also known as linear classifiers (LC), and second order polynomial classifier, known as binomial classifier (BC), were designed and their performance was evaluated with nonparametric detection.

4.3.1 System Parameters

The simulation setup of the CR network including primary transmitted signal, channel, CR receivers, and the base station parameters are specified as follows. The network consists of N cognitive users who contribute in making the global decision at the CR base station, where $N \in \{1,3,5\}$ users. Each CR extracts a local decision variable d_i, based on the detection scheme implemented. Both linear classifier and second order polynomial classifier models were developed for deciding on the vacancy of the spectrum at the frequency band of interest.

The primary signal is assumed to follow a linearly modulated signal model described in (3.1). Specifically, the primary signal is modeled as a BPSK signal which is down converted into baseband, over which the features are extracted. The signal's data rate considered is $R_b = 100\text{kbps}$. A flat slow Rayleigh fading channel is considered for the channel model with a coherence time $T_c = 20T_b$, where $T_b = \frac{1}{R_b}$. CRs are assumed to experience AWGN channel with variance ${\sigma_n}^2 = 1$. The i^{th} CR

receives a signal with signal-to-noise ratios SNR_i that differs according to the CR's proximity from the primary user. The SNR_i follows a normal distribution with a variance $\sigma^2 = 4$ dB and mean equivalent to SNR_{avg}, emulating a log normally distributed loss path, to account for the large scale fading. The detector's structures based on energy and autocorrelation are implemented with the following parameters. The sampling frequency at the receivers is $f_s = 4f_{max}$, where $f_{max} = R_b$ for the down converted signal satisfying the Nyquest condition to recover an alias-free signal. The observation window size for is varied for energy detection to investigate the tradeoff in performance between fast decision making and more reliable performance over a longer decision interval. The simulation environment was developed using the above settings to generate classifier's training and testing data sets.

4.3.2 Simulation Results

The performance of the designed classifiers is evaluated as novel input data is subjected to the models. Energy detection is performed at the various secondary users and the extracted decision variables are provided to the recognition model at the CR base station. The probability of detection achieved by the recognition system at different average received signals levels is presented in Figure 4.4 for different numbers of users cooperating in decision making at the base station. The results are obtained such that a target false alarm (P_f) of 10% is achieved.

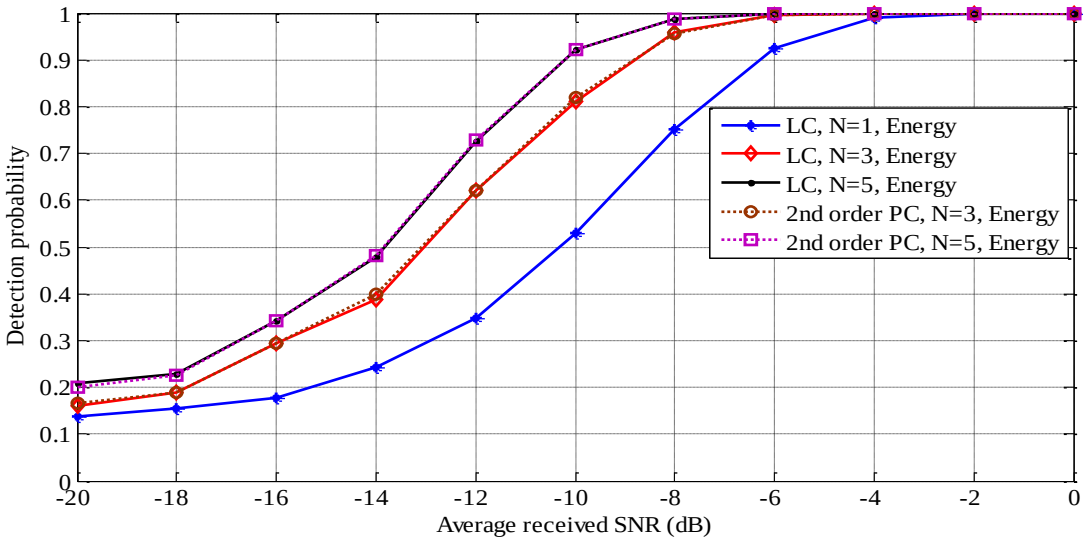

Figure 4.4. Detection performance of the proposed cooperative LC and 2nd order PC with energy based feature extraction at P_f=10% and observation window M=200 bits.

As observed, the second order polynomial classifier does not improve the detection probability performance as compared to the first order linear classifier. However, the second order polynomial classifier requires more memory and computational complexity to perform the expansion operation as opposed to the linear classifier. Hence, the linear classifier is chosen as the optimal model since an appropriate performance is obtained with the minimum required memory space and computational cost resulting in faster decision speed. Moreover, the advantage of cooperative sensing compared to single radio based sensing is observed in the detection performance improvement as the number of secondary users contributing to signal classification is increased. A received SNR of around -9 dB is appropriate to reach a detection probability of 90% with 3 CRs, while a received signal with an average SNR of around -6.5 dB is required to achieve the same detection rate with 1 CR, resulting in gain of 2.5 dB. As the number of receiver collaborating in global decision increases, the enhancement in performance diminishes, posing an upper limit on the possible gain by increasing cooperating nodes.

Further, performance improvements can be realized through increasing the observation window size. The results of energy detection for a received signal with $\mathrm{SNR}_{\mathrm{avg}} = -5$ dB, $N = 3$ users, and $P_f = 10\%$, are depicted in Figure 4.5 for both linear and second order polynomial models. It is evident that almost a 100% detection rate is possible with energy detection at $\mathrm{SNR}_{\mathrm{avg}} = -5$ dB, with a window size greater than 100 bits. Hence, longer observation windows may result in higher detection rates with smaller SNRs at the expense of decision making speed.

A very informative performance measure in CR networks is the receiver operational characteristics (ROC) curve. ROC curves represent the probability of detection as the target false alarm varies at certain operational parameters. Typically, ROC curves of a system are generated through off-line calibration processes, where the threshold is varied to achieve different false alarm rates. Thereupon, the probability of detection is measured at each false alarm probability. To further illustrate detection performance of linear classifier, the ROC is obtained when primary signal is received with $\mathrm{SNR}_{\mathrm{avg}} = -14$ dB and observation window size of $M = 200$ bits. The ROC curves are shown in Figure 4.6.

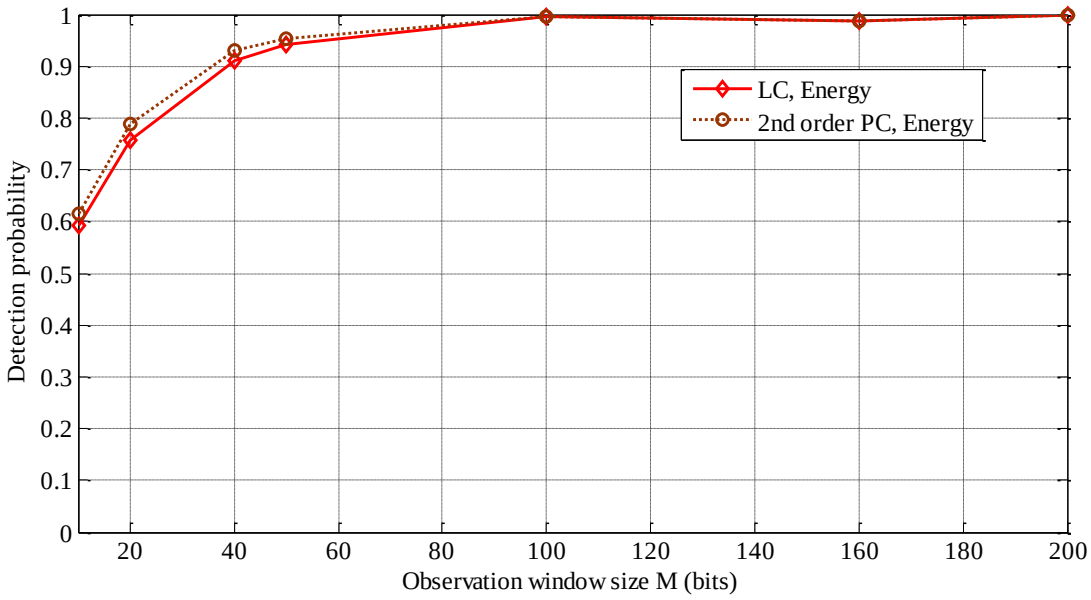

Figure 4.5. Detection performance of cooperative LC and 2nd order PC with energy based feature extraction as M is varied at $\mathrm{SNR}_{\mathrm{avg}} = -5\mathrm{dB}$, $N = 3$ users, and $P_f = 10\%$.

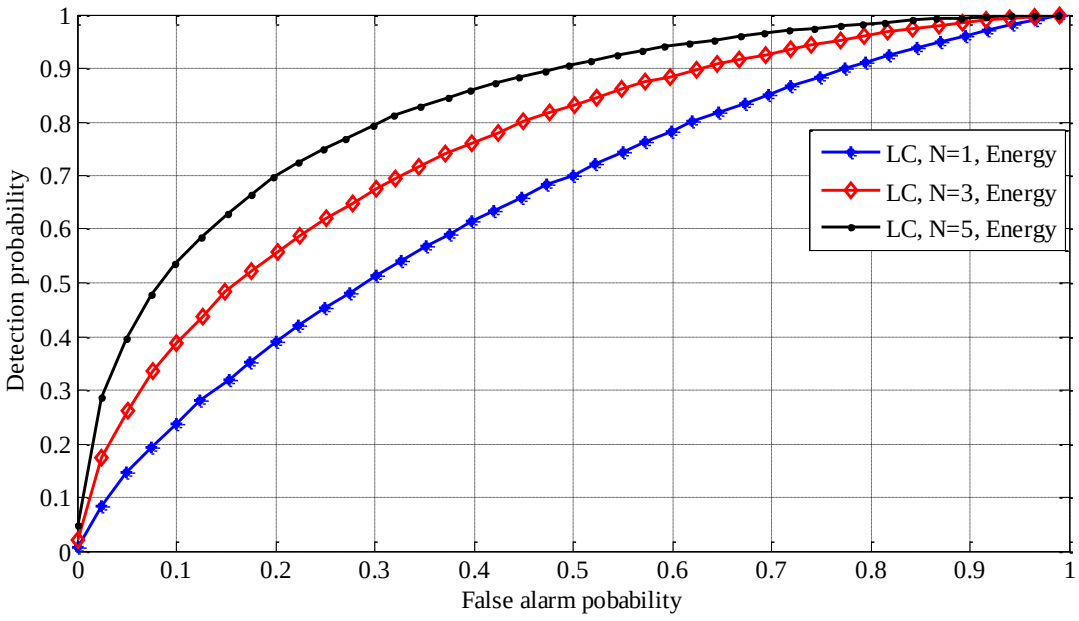

Figure 4.6. The ROC curves of the proposed LC with energy based feature extraction at $\mathrm{SNR}_{\mathrm{avg}} = -14\mathrm{dB}$ and $M = 200$ bits.

From Figure 4.6, it is seen that the detection probability deteriorates for low false alarm rates and improves as higher false alarm probability is tolerable. In order to achieve low false alarm rate, the threshold level needs to be raised. Raising the threshold level above classifier's output score, corresponding to occupied spectrum

class, may lead to miss detecting primary signal's presence; and consequently causing more interference to the primary network's users . It can be noted that higher detection is accomplished with higher number of cooperating CRs. Achieving maximum spectral utilization corresponding to 0% false alarm rate at $\mathrm{SNR}_{\mathrm{avg}} = -14$ dB will lead to miss detecting any received signal and hence constantly causing interference to primary users. A 90% detection probability is possible for energy detection with 50% spectral utilization when the number of cooperating users is 5. Additionally, to maintain detection rate above 90%, false alarm rate cannot be lower than 60% and 80% when the number of CRs is 3 and 1, respectively.

The performance of the classification system is then tested with the autocorrelation based detection technique to extract features from novel testing data. Figure 4.7 represents the performance of linear classifier against second order polynomial classifier as the received average SNR is varied, while keeping a target false alarm probability of 10%. The decision variable in the autocorrelation detector is estimated over a sensing window with $M = 200$bits, which is divided into $B = 10$ subsections, over which autocorrelation is calculated as discussed earlier in this chapter. It is noticeable that still the linear classifier performs comparable to the second order polynomial classifier with lower complexity when the autocorrelation detection is implemented. The achievable gain, as the cooperative CRs increase from 3 to 5 users, is smaller than that obtained as we move from 1 to 3. The improvement gain decreases from around 2.5 dB to 1 dB as the number of receivers increases.

Moreover, Figure 4.8 shows the ROC curves for autocorrelation detection with different number of CRs at a received signal level of –14 dB. It is apparent that there is a performance enhancement as different number of CRs collaborates in making the decision increases. Finally, Figure 4.9 shows the detection performance with observation window size of $M = 140$ bits as the number of subsections, over which the autocorrelation is computed, varies. It is clear that increasing the number of subsections decreases the detection performance since the number of samples used in the estimation of autocorrelation decrease. Hence, smaller number of subsections, that satisfies the condition of constant channel gains over one window, is preferable.

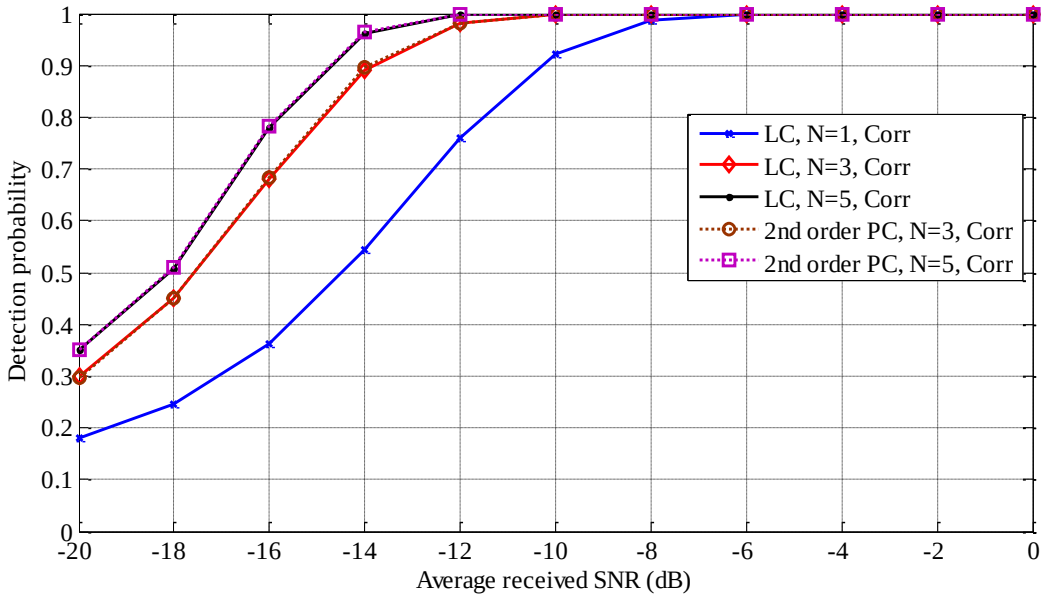

Figure 4.7. Detection performance of the proposed cooperative LC and 2nd order PC with autocorrelation based feature extraction at P_f=10% and observation window M=200 bits.

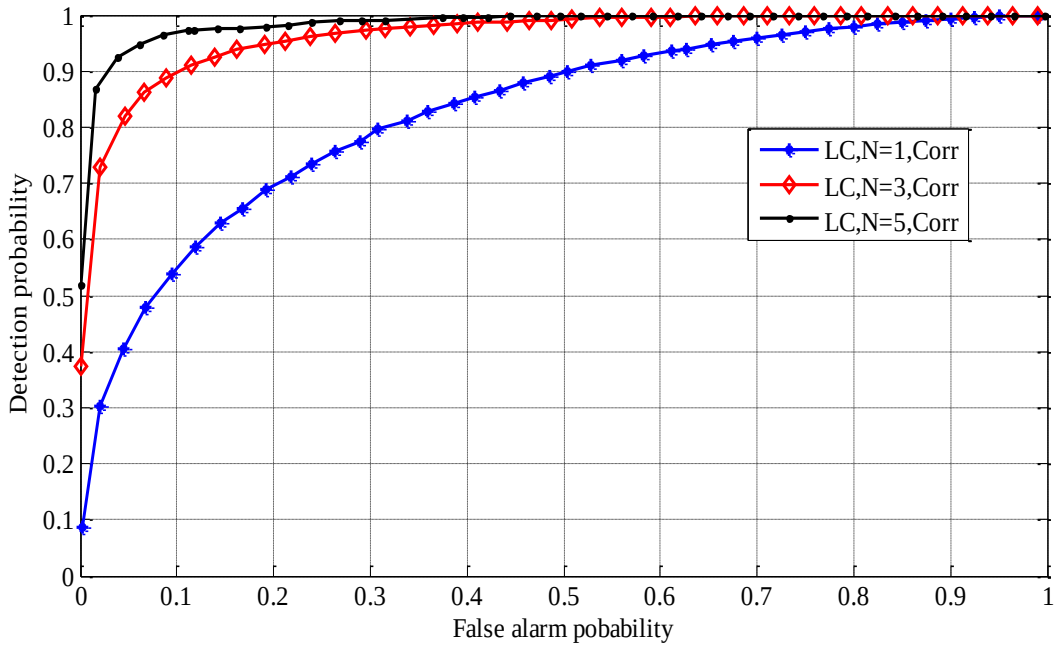

Figure 4.8.The ROC curves of the proposed LC with autocorrelation based feature extraction at $\mathrm{SNR}_{\mathrm{avg}} = -14\mathrm{dB}$ and $M = 200$ bits.

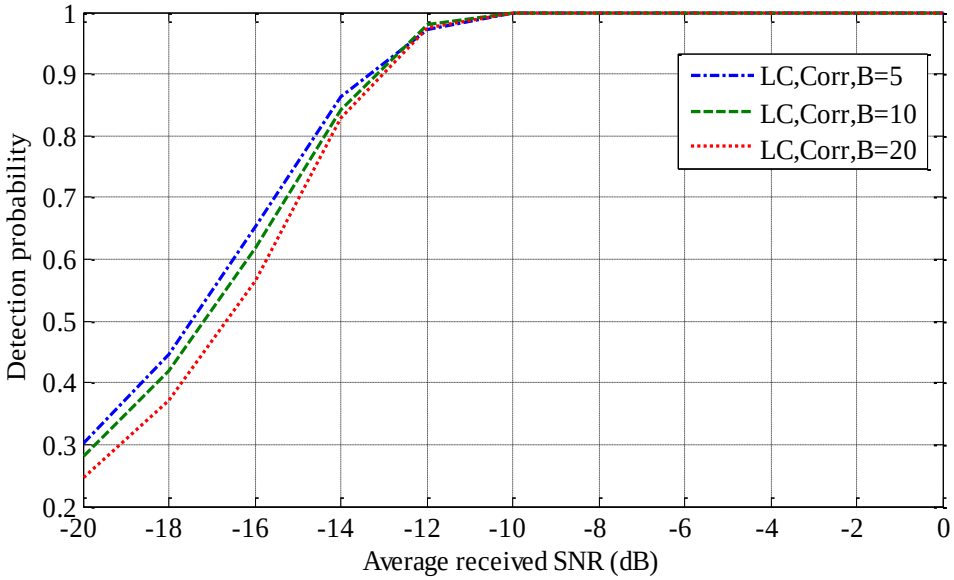

Figure 4.9. Detection performance of the proposed cooperative LC with autocorrelation based feature extraction at P_f=10% and observation window M=140 bits.

4.4 Discussion of Results

In light of presented results, it is evident that energy detection is capable of providing a 100% detection rate at SNR_{avg} above -7 dB, and can be maintained above 90% for smaller values of SNR_{avg} . However, we compare the performance of energy detection and autocorrelation detection in terms of probability of detecting spectrum holes, while satisfying a condition on spectral utilization. Our results indicate that adopting autocorrelation detection yields superior performance over energy detection under same conditions. A comparison of energy and autocorrelation approaches in the classifier model is demonstrated in Table 4.1 and

Table 4.2. For instance, a detection probability of 100% can be achieved by autocorrelation detector at $\text{SNR}_{\text{avg}} = -12\text{dB}$, while a signal level of -7 dB is required to achieve the same performance by energy detector with $N = 5$. Moreover, autocorrelation detection performs much better than energy detection, when high spectral utilization is required (small false alarm rate). In order to achieve 1% false alarm rate, a detection performance of 74% is obtained using autocorrelation scheme whereas energy scheme can detect primary signal up to 15% of the time only, under the same conditions. The higher and more reliable performance of autocorrelation comes at the expense of higher receiver complexity required in autocorrelation estimation, as opposed to the simple energy detector.

The performance is also highly affected by the window size over which the local decision variables are estimated. As the window size increases, the data used for training and testing becomes more representative to the present signal in the spectrum, and hence the classifier's output score is more accurate. However, the larger the window size is, the longer it takes for decision making of spectrum availability by the classifier at the base station. This yields a delay in spectral allocation when the spectrum is available; hence, resulting in lower spectral utilization.

The demonstrated results show that there is an optimal window size with a specific constraint on false alarm rate and received signal level at which the detection probability is maximized. In other words, increasing sensing window size above that value no longer improves detection probability. Consequently, sensing time can be varied to optimize detection probability according to the received signal SNR level. As a high signal level is received, smaller window size is adopted such that faster decisions are made with high detection rate, and vice versa.

Table 4.1. Detection probability of energy and autocorrelation detectors at $\mathrm{SNR} = -14\mathrm{dB}$ with various number of receivers and different P_f.

		$P_f = 1\%$		$P_f = 10\%$		$P_f = 20\%$	
		$N = 3$	$N = 5$	$N = 3$	$N = 5$	$N = 3$	$N = 5$
Detection probability	Energy	8.2%	15%	38.7%	48%	55.6%	70%
	Autocorrelation	55.6%	74.4%	89.5%	96.4%	95%	98.1%

Table 4.2. Detection probability of energy and autocorrelation $P_f = 10\%$ with various number of receivers and different SNR.

		$\mathrm{SNR} = 0\mathrm{dB}$		$\mathrm{SNR} = -10\mathrm{dB}$		$\mathrm{SNR} = -20\mathrm{dB}$	
		$N = 3$	$N = 5$	$N = 3$	$N = 5$	$N = 3$	$N = 5$
Detection probability	Energy	100%	100%	82%	92.1%	16%	20%
	Autocorrelation	100%	100%	99.9%	100%	29.6%	35%

The tradeoff between spectral utilization and interference avoidance with coexisting primary network can be visualized from the ROC curves of both schemes. At high false alarm rates, a high detection probability is achieved, repressing low spectral utilization as well as less interference with primary users. In other words, the number of times the system decides in favor of the hypothesis H_1 , while the null hypothesis H_0 is true is large; denying the secondary users from utilizing the available channel. However, large false alarm rates reduce the interference with primary users, resulting in high detection probabilities.

4.5 Conclusions

Nonparametric spectrum sensing was considered as the practical signal detection approach when information on primary users is not accessible. The performance of nonparametric detection schemes was evaluated, when they are utilized in extracting input features to the proposed classification system. The presented results justified the capability of the proposed pattern recognition system to detect the presence of primary signals as nonparametric features are subjected to it. Moreover, we illustrated the impact of utilizing spatial diversity, via cooperative sensing, in enhancing the detection probability at a fixed false alarm rate. Both linear and second order polynomial classifiers were implemented for detecting spectral availability. It was shown that the linear classifier performs comparably to the second order polynomial classifier. Therefore, linear classifier represents an optimal classifier model as it requires less computational cost compared to second order polynomial classifier with equal number of receivers. Finally, results indicated that autocorrelation based feature extraction outperforms energy based feature extraction.

CHAPTER 5

PARAMETRIC SPECTRUM SENSING

In this chapter, parametric spectrum sensing detectors are described and analyzed. In section 5.1, principles of cyclostationary feature detection are discussed and the cyclic spectrum periodogram is outlined, followed by a brief review of coherent based detection as it is utilized in spectrum sensing in section 5.2. In section 5.3, a generic system model is developed where the parametric feature extraction schemes are applied to the trained classifier models. Finally, simulation results of the first and second order polynomial classifiers' performances, as parametric features are subjected to them are discussed.

5.1 Cyclostationary Feature Detection

Most of the work analyzing the significance of spectral redundancy present in cyclostationary communications signals was first developed by Gardner and his colleagues [35][36]. Thereafter, cyclostationary feature detection has been adopted for different purposes including spectrum sensing, classification [37], synchronization, signal detection [13] and equalization [38][13]. In this section, analysis of cyclostationary feature detection is provided, including a discussion of cyclic autocorrelation function (CAF) and spectral correlation density (SCD) computations.

5.1.1 Cyclic Autocorrelation Function (CAF)

Most communication signals can be modeled as cyclostationary random processes, as they are usually characterized by built-in periodicities in their mean and autocorrelation. These underlying periodicities arise as a result of coupling stationary message signals with sinusoidal carriers, repeating spreading codes, pulse trains or cyclic prefixes. These periodicities may also take place due to sampling and multiplexing of the message signal during the generation process. A zero-mean

process $x(t)$ is said to be cyclostationary in the wide sense if both its mean and autocorrelation exhibit periodicity in time [17]:

$$m_x(t+T_0) = m_x(t) \tag{5.1}$$

$$R_x\left(t+\frac{\tau}{2}, t-\frac{\tau}{2}+T_0\right) = R_x\left(t-\frac{\tau}{2}, t+\frac{\tau}{2}\right) \tag{5.2}$$

where the period of the mean and autocorrelation is T_0. Moreover, $m_x(t)$ and $R_x(t)$ are defined as:

$$m_x(t) = \mathrm{E}[x(t)] \tag{5.3}$$

$$R_x\left(t-\frac{\tau}{2}, t+\frac{\tau}{2}\right) = \langle x\left(t+\frac{\tau}{2}\right) x^*\left(t-\frac{\tau}{2}\right)\rangle \tag{5.4}$$

where $\langle . \rangle$ is the time averaging operation $\langle . \rangle = \lim_{T_0\to\infty} \frac{1}{T_0}\int_{-T_0/2}^{T_0/2}(.)dt$. Another definition of second order periodicity is given as follows: A signal $x(t)$ contains second order periodicity if and only if the Fourier transform of its autocorrelation has discrete spectral lines at non-zero frequencies $\alpha \neq 0$ [36][35]:

$$R_x^{\alpha}(\tau) \triangleq \langle x\left(t+\frac{\tau}{2}\right) x^*\left(t-\frac{\tau}{2}\right) e^{-j2\pi\alpha t}\rangle \neq 0 \tag{5.5}$$

where $\boldsymbol{\alpha} \in \{0, \pm 1/T_0, \pm 2/T_0, \ldots\}$. $R_x^{\alpha}(\tau)$ is considered as the second order periodicity fundamental parameter, which represents the Fourier coefficients of additive sine wave components contained in the delay product $x\left(t+\frac{\tau}{2}\right)x^*\left(t-\frac{\tau}{2}\right)$ at frequencies $\boldsymbol{\alpha}$. The notation $R_x^{\alpha}(\tau)$ is chosen to denote this parameter, since it reduces to the conventional autocorrelation function $R_x(\tau)$, defined in (5.2), at frequency $\alpha = 0$.

R_x^{α} is called the cyclic autocorrelation function(CAF), since it is the generalization of the autocorrelation function in which sinusoidal (cyclic) weighting coefficients are included before the time averaging is carried out. The autocorrelation of a signal and the CAF are used to distinguish between two types of signals, namely stationary and cyclostationary. Signals whose CAF exist and has non-zero values only at $\alpha = 0$ ($R_x^{\alpha}(\tau) = 0$ for any $\alpha \neq 0$) are said to be purely stationary signals. However, signals with CAF existing at frequencies other than zero ($R_x^{\alpha} \neq 0$ for any $\alpha \neq 0$) are called cyclostationary signals of second order [35][36]. Any non-zero value for the

frequency parameters α, at which the CAF is non-zero, is called a cycle frequency. Furthermore, the cycle spectrum is the discrete set of cycle frequencies.

Another interpretation of CAF can be realized by factoring $e^{-j2\pi\alpha t}$ in (5.3) and rewriting it as follows:

$$R_x^\alpha(\tau) = \langle \left[x\left(t+\frac{\tau}{2}\right)e^{-j\pi\alpha\left(t+\frac{\tau}{2}\right)}\right]\left[x\left(t-\frac{\tau}{2}\right)e^{j\pi\alpha\left(t-\frac{\tau}{2}\right)}\right]^* \rangle \quad (5.6)$$

As shown in (5.6), the CAF can be considered as the conventional cross-correlation function between two signals $v(t)$ and $u(t)$:

$$R_x^\alpha(t;\alpha) = R_{uv}(\tau) = \langle v\left(t-\frac{\tau}{2}\right)u^*\left(t+\frac{\tau}{2}\right)\rangle \quad (5.7)$$

where

$$u(t) = x(t)e^{-j\pi\alpha t} \quad (5.8a)$$

$$v(t) = x(t)e^{+j\pi\alpha t} \quad (5.8b)$$

where $u(t)$ and $v(t)$ represent frequency shifted versions of the signal $x(t)$ by $\pm\alpha/2$. Therefore, a signal $x(t)$ exhibits second order cyclostationarity if and only if its frequency translates $u(t)$ and $v(t)$ are correlated for some $\alpha \neq 0$.

5.1.2 Spectral Correlation Density (SCD)

As it is useful in many applications to determine the spectral characteristics of stationary signals, localizing the cyclic autocorrelation (CAF) in frequency provide comprehensive means of examining cyclostationarity of a signal. Cyclostationarity of a signal leads to the presence of specific patterns in the spectrum of the signal, which can be examined using the so called spectral correlation density function (SCD) [36][38]. By analogy to computing the power spectral density of a stationary signal using its autocorrelation, the SCD of a cyclostationary signal is the Fourier transform of its CAF [36]:

$$S_x^\alpha(f;\alpha) = \int_{-\infty}^{\infty} R_x^\alpha(\tau)e^{-j2\pi f\tau}\,d\tau \quad (5.9)$$

Another way of expressing SCD can be interpreted from (5.6) as follows [7]:

$$S_x^{\alpha}(f;\alpha) = \lim_{T\to\infty}\lim_{\Delta t\to\infty}\frac{1}{T\Delta t}\int_{-\frac{\Delta t}{2}}^{\frac{\Delta t}{2}} X_T\left(t, f+\frac{\alpha}{2}\right) {X_T}^*\left(t, f-\frac{\alpha}{2}\right) dt \tag{5.10}$$

where;

$$X_T(t,l) = \int_{t-\frac{T}{2}}^{t+\frac{T}{2}} x(m)\, e^{-j2\pi ml}\, dm \tag{5.11}$$

is the complex envelope of the spectral component of $x(t)$, $\Delta f = 1/T$ represents the frequency resolution and Δt is the averaging time over which the SCD is estimated. It is clear from (5.10) that SCD represents the temporal correlation of the filtered frequency translates of $x(t)$. In other words, S_x^{α} describes the correlation of the amplitude and phase fluctuations of the narrow band spectral components of $x(t)$ centered at frequencies $f \pm \frac{\alpha}{2}$ as the bandwidth $\Delta f = 1/T$ approaches zero. Therefore, an ideal implementation of (5.10) is obtained by allowing the averaging time Δt to approach infinity and spectral resolving bandwidth Δf approaches zero [36]. Consequently, in order to have a reliable estimation of SCD with finite parameters, the temporal-spectral resolution product is required to greatly exceed unity [13]:

$$\Delta f \Delta t \gg 1 \tag{5.12}$$

In order to meet the above conditions in practical implementations, discrete frequency-smoothing formulation of the above cyclic periodogram is defined [39]:

$$S_x^{\alpha}[k] = \frac{1}{P}\sum_{v=-\frac{P-1}{2}}^{\frac{P-1}{2}} \frac{1}{\Delta t} X\left(t, k+\frac{\alpha}{2}+vf_s\right) X^*\left(t, k-\frac{\alpha}{2}+vf_s\right) W(v) \tag{5.13}$$

where

$$X(t,k) = \sum_{n=0}^{M-1} x[n] e^{-j2\pi kn/M} \tag{5.14}$$

M is the number of samples over which the spectrum of the received signal $x[k]$ is calculated (FFT length), $\Delta f = P/\Delta t$ is the spectral smoothing interval's width, T_s is the time sampling increment, $f_s = 1/T_s$ is the sampling rate, $\Delta t = MT_s$, and P is the number of frequency bins that are averaged together using a frequency smoothing window $W(v)$, such as rectangular and hamming smoothing windows. In order to satisfy the condition in (5.12), the resolution product $\Delta f \Delta t = \frac{P}{\Delta t}\Delta t = P \gg 1$. Hence, for a given averaging time Δt, a larger number of frequency averaging bins is required for reliable SCD estimation. Moreover, it is clear from $\Delta f = P/\Delta t$ that greater observation time is required for smaller spectral resolution and consequently better SCD estimation.

5.2 Coherent Detection

Another parametric based sensing scheme investigated in this work is the coherent detection. Coherent detection maximizes the received signal-to-noise ratio by using match filtering, resulting in high detection probability. Optimally, coherent detection is performed by demodulating primary user's signal, which requires a priori information of the primary signal including modulation type, pulse shaping, packet format, control and synchronization preambles [40]. Preamble patterns can be utilized by mobile terminals within a given mobile network to identify transmitting base stations within their area. Moreover, control information provides commands and other instructions for decoding received signals.

If the synchronizing preamble patterns are known at the cognitive network end, coherent sensing can be exploited by correlating the incoming signal with the known patterns. This is effectively correlating the signal with itself resulting in an autocorrelation function that peaks at a delay $k = 0$, in the presence of signal [18]. However, when only noise is present the correlation will be equivalent to cross-correlation between a stationary signal with the preamble pattern which are uncorrelated and hence will result in no peak at a delay $k = 0$. Therefore correlating the received signal with a known preamble pattern will result in discriminative features for the classifier model. The decision variable of correlation is given by:

$$y[k] = Re\left[\sum_{n=0}^{M-1} x[n]s^*[n-k]\right] \text{ for } k = 0, \pm 1, \pm 2, \ldots \quad (5.15)$$

where $s^*[n]$ is the conjugate of the known signal pattern, $x[n]$ is the received signal, and M is the number of samples over which the correlation is performed. The structure of the coherent detector is further discussed in the following section.

5.3 Proposed Parametric Cooperative System Model

We present a model for a cooperative CR network where secondary users are assumed to have prior information about the primary users. Prior information includes knowledge of primary user's carrier frequency and preamble synchronizing patterns. We therefore examine both cyclostationary feature detection and coherent detection techniques to extract discriminative feature as input to the classifiers. The block diagram in Figure 5.1 shows the proposed parametric based spectrum sensing algorithm.

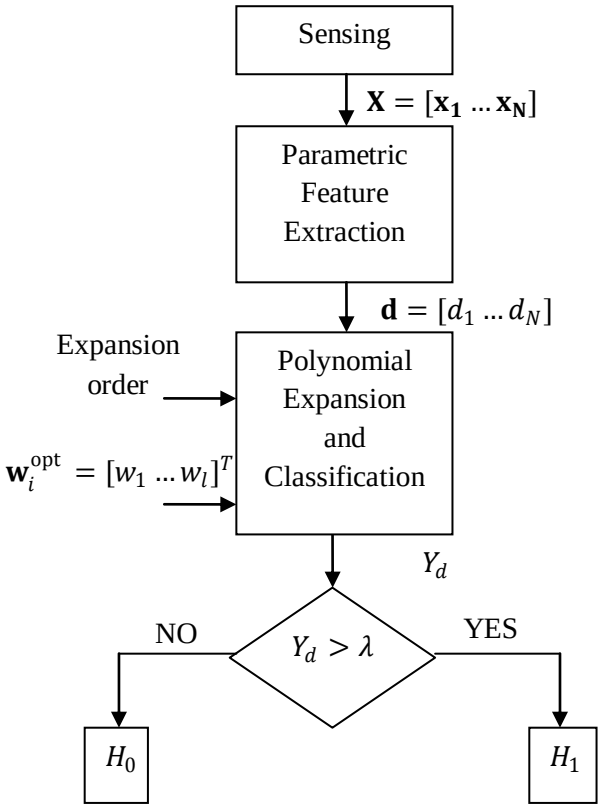

Figure 5.1. Parametric spectrum sensing algorithm.

The steps of the algorithm are as follow:

1) The received signal at each CR is measured over a period of time at a sampling rate of f_s samples/second.

2) A parametric feature extraction is performed at each cooperative secondary user. The input to the feature extraction block $\mathbf{X}$ consists of N data sequences, $\mathbf{x_i}$ each of length M bits. The received sequence $\mathbf{x_i}$ is used to extract a feature, also referred to as local decision variable, d_i by the i^{th} CR. Hence, the N secondary users provide an input feature vector $\mathbf{d} = [d_1 \dots d_N]$ to the CR base station.

3) The local decision variables are then transmitted to the CR base station for decision making. The decision variables are fed to a trained polynomial classifier with model parameter $\mathbf{w}_1^{opt}$, representing occupied spectrum.

4) A global decision is then made about the vacancy of the spectrum by comparing the classifier's output y_1 to the threshold that was pre-calculated to achieve a target false alarm rate (for more details, refer to section 3.3.4) .

The signal model introduced in (3.1) is adopted in parametric sensing. We consider a BPSK primary transmitted signal $s(t)$. In coherent detection (CD), the signal is down converted into its baseband equivalent $s_{\text{coh}}(t)$ modeled by:

$$s_{\text{coh}}(t) = \sum_k \sqrt{E_b} d_k h(t - kT_b) \tag{5.16}$$

where E_b is the average energy per bit, T_b is the average bit duration, $h(t)$ is the pulse shape, and $d_k \in \{-1,1\}$. In cyclostationary feature detection (CFD), on the other hand, we process the received bandpass primary signal instead of its baseband equivalent. The bandpass is used such that we preserve the underlying periodicity in the primary signal, caused by the modulating carrier, and exploit them in cyclostationary feature detection. The received BPSK bandpass signal $s_{\text{cyc}}(t)$ with carrier frequency f_c is modeled by

$$s_{\text{cyc}}(t) = Re\left[\sum_k \sqrt{E_b} d_k h(t - kT_b) . e^{-j2\pi f_c t}\right] \tag{5.17}$$

In parametric spectrum sensing, the feature extraction block structure depends on the available prior information to the cognitive network. The detectors' structures investigated in this research are explained next.

5.3.1 Cyclostationary Based Feature Extraction

In this research, when cyclostationary detection is adopted as the feature extraction technique in spectrum sensing, the cyclic periodogram introduced in 5.1.2 is applied. The transmitted signal is assumed to be a BPSK signal $s_{\text{cyc}}(t)$ as defined in (5.17). The SCD can be thought of a cross-correlation function between the spectral translates of the signal at $f \pm \frac{\alpha}{2}$, for some cyclic frequency α. The SCD estimation periodogram is implemented to obtain the cyclic feature extraction receiver structure as shown in Figure 5.2.

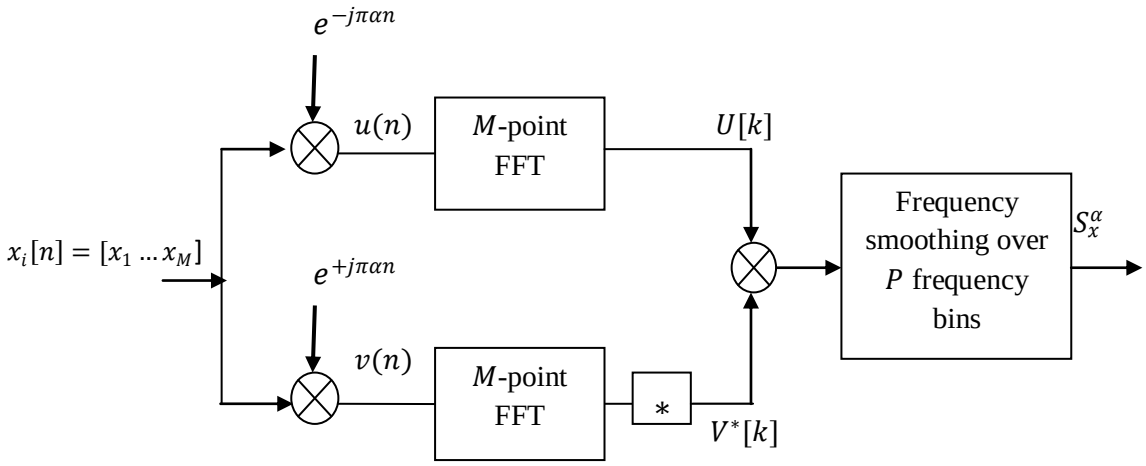

Figure 5.2. Block diagram of cyclostationary based feature extraction.

Based on Figure 5.2, cyclostationary detection can be conducted through the following steps:

1) Given a received signal $x(t)$, it is sampled at a rate of f_s to obtain the received signal described in (3.1). Thereafter, each M samples, $x_i[n] = [x_{i1} \dots x_{iM}]$, are fed to the detector at the i^{th} receiver.

2) The input $x_i[n]$ is then multiplied by $e^{\pm j\pi\alpha n}$ in order to produce the frequency translates of $x_i[n]$, namely $v[n]$ and $u[n]$.

3) The M-point FFT is next calculated for the frequency shifted versions of $x_i[n]$ in order to obtain their frequency spectrum as follow:

$$U[k] = \frac{1}{\sqrt{M}} \sum_{n=0}^{M-1} x_i[n] e^{-j\pi\alpha n} \, e^{-\frac{j2\pi kn}{M}} = X_i\left[k + \frac{\alpha}{2}\right] \quad (5.18)$$

$$V[k] = \frac{1}{\sqrt{M}} \sum_{n=0}^{M-1} x_i[n] e^{+j\pi\alpha n} \, e^{-\frac{j2\pi kn}{M}} = X_i\left[k - \frac{\alpha}{2}\right] \quad (5.19)$$

4) The SCD is computed by first finding the spectral correlation of the input's frequency translates. The output of correlation is then spectrally smoothed using a frequency smoothing window W with P frequency averaging bins. The SCD is then given by:

$$S_x^{\alpha}[k] = \frac{1}{P} \sum_{v=-\frac{P-1}{2}}^{\frac{P-1}{2}} \frac{1}{\mathrm{M}} U[k+v] V^*[k+v] W(v)$$

$$= \frac{1}{P} \sum_{v=-\frac{P-1}{2}}^{\frac{P-1}{2}} \frac{1}{\mathrm{M}} X_i\left[k + \frac{\alpha}{2} + v\right] X_i{}^*\left[k - \frac{\alpha}{2} + v\right] W(v) \quad (5.20)$$

5) The process is repeated for each M received samples.

The decision variable d_i is then defined as the value of SCD at $k = 0$ representing the peak of cyclic frequency spectrum when a primary signal is present. After the SCD estimation, the received signal model changes from that given by (3.1) depending on the received hypothesis, for constant channel gains:

$$S_x^{\alpha_0}[k] = \begin{cases} |g|^2 \, S_s^{\alpha_0}[k] + S_n^{\alpha_0}[k] \; : & H_1 \\ S_n^{\alpha_0}[k] \; : & H_0 \end{cases} \quad (5.21)$$

where $S_n^{\alpha_0}[k]$ represents the SCD of the AWGN at some cyclic frequency $\alpha = \alpha_0$ when no signal present; while $S_s^{\alpha_0}[k]$ is the SCD of the transmitted primary signal. Since the AWGN is a wide sense stationary process and does not possess second order cyclostationarity, it will not have a peak at any cyclic frequency $\alpha = \alpha_0$. On the other hand, the bandpass BPSK signal exhibits second-order cycle frequencies at $\frac{\alpha_0}{2} = f_c + \frac{m}{T_{\text{symbol}}}$ [2][9], for some integer $m = 0, \pm 1, \pm 2, \ldots$. T_{symbol} represents the symbol

duration and for BPSK is equivalent to the bit duration T_b. Since the strongest spectral lines of a BPSK signal appear at $f = \pm f_c$, the strongest cyclic components are observed at $\frac{\alpha_0}{2} = \pm f_c$ [9]. For illustration, the PSD of a BPSK signal's frequency translates are given in Figure 5.3 and Figure 5.4, respectively, where the sampling frequency for this example is $f_s = 10 f_c$ Further, the SCD of both the BPSK signal and AWGN are presented in Figure 5.5 and Figure 5.6, respectively.

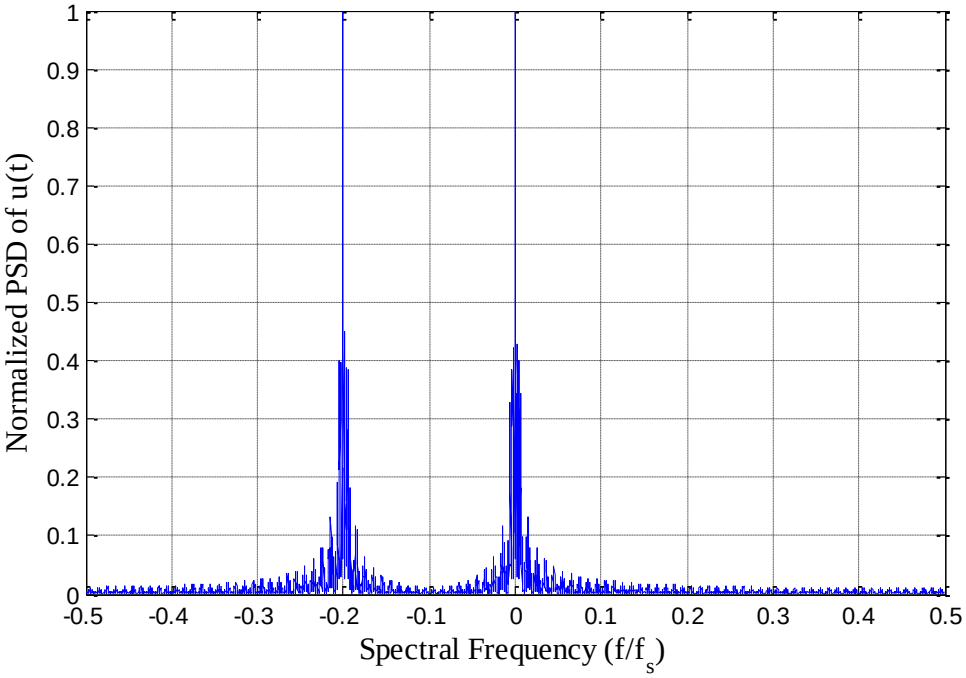

Figure 5.3. Power spectral density of the frequency translate $u(t)$ at $\frac{\alpha_0}{2} = f_c$.

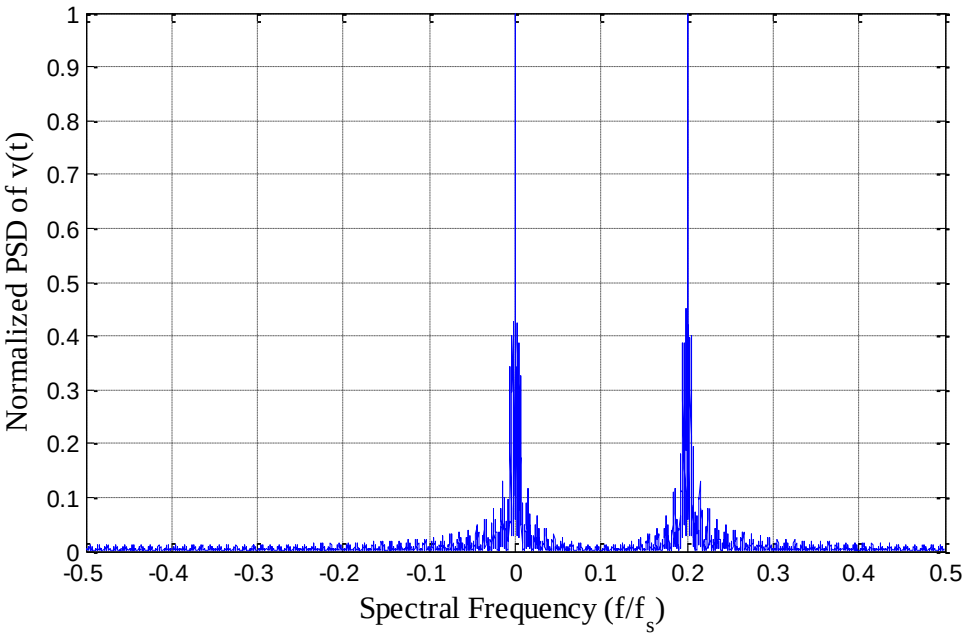

Figure 5.4. Power spectral density of the frequency translate $v(t)$ at $\frac{\alpha_0}{2} = f_c$.

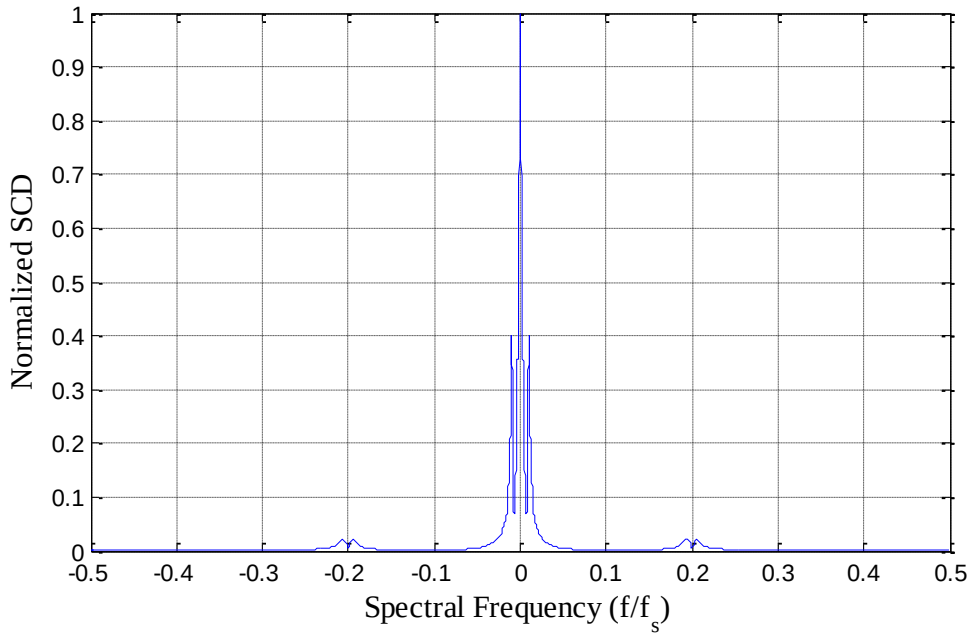

Figure 5.5. SCD of BPSK signal at cycle frequency $\frac{\alpha_0}{2} = f_c$.

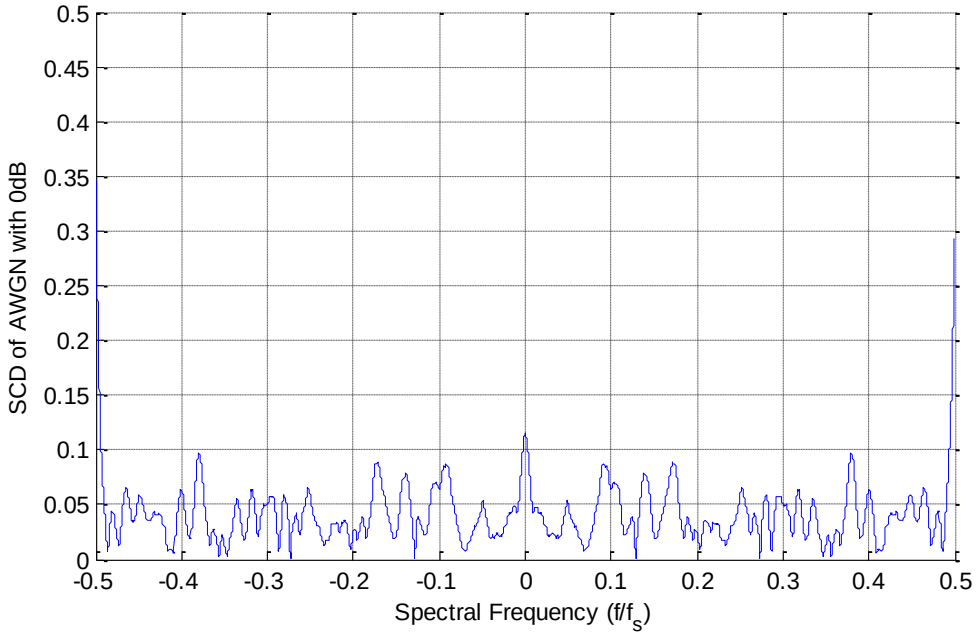

Figure 5.6. SCD of AWGN at cycle frequency $\frac{\alpha_0}{2} = f_c$.

As shown in the above figures, the SCD of BPSK signal for $\frac{\alpha_0}{2} = f_c$ contains a clear peak at spectral frequency $\frac{f}{f_s} = 0$, which does not occur in the SCD of AWGN. Therefore, the local decision variable for cyclostationary detection can be chosen to be $S_x^{\alpha_0}[0]$, representing a discriminative feature as input to the classifier:

$$d_i = S_x^{\alpha_0}[0] = \begin{cases} |g|^2 S_s^{\alpha_0}[0] + S_n^{\alpha_0}[0] & : \quad H_1 \\ S_n^{\alpha_0}[0] & : \quad H_0 \end{cases} \tag{5.23}$$

Finally, similar to the case of autocorrelation, the SCD is estimated over multiple subsections of the observation window. The length of the subsections is chosen to be close to the estimated coherence time of the channel, such that (5.23) is valid; i.e. $E[|g|^2] = |g|^2$.

5.3.2 Coherent Based Feature Extraction

In coherent detection, the transmitted primary signal $s_{\text{coh}}(t)$ was defined in (5.16). Primary users are assumed to be using time division multiple access (TDMA), with a frame size M bits and a synchronizing preamble at the beginning of each frame with length L bits. The preamble sequence is pre-known at secondary receivers. The cognitive users will be acquiring data for L bits, or equivalently a sensing duration $\Delta t = LT_s$, every M bits. Thus, the transmitted primary signal available for coherent sensing is shown in Figure 5.7, where the dashed blocks represent the segment of the incoming frame at which CRs acquire sensing data.

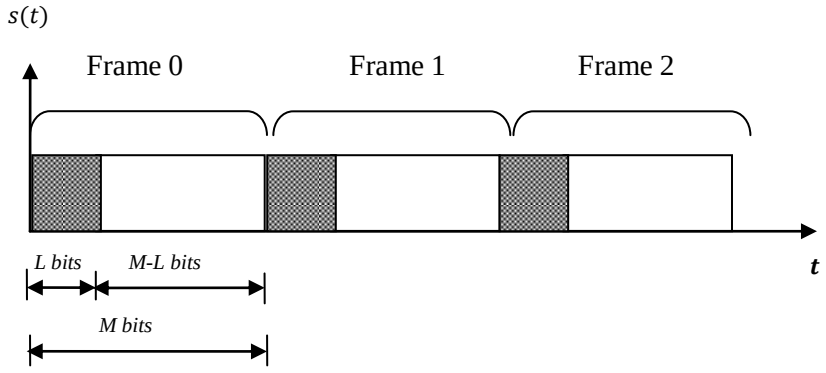

Figure 5.7. Sensing data blocks within a segment of the incoming signal frames.

The coherent based detection algorithm assuming L bits-length preamble is outlined as follows:

1) The received signal $x_i(t)$, illustrated by Figure 5.7, is applied to a gating function, where signal is acquired only for the pre-known preamble duration. The acquired gated data is sampled at f_s samples/second to obtain the preamble sampled signal $x_{\mathrm{g}}[n] = \{x[1] \dots x[L]\}$.

2) Thereafter, the acquired gated signal is correlated with the preamble sequence s_{p} as follows:

$$R_{xs}[k] = Re\left[\sum_{n=1}^{L} x_{\mathrm{g}}[n]\mathrm{s}^{*}{}_{\mathrm{p}}[n-k]\right] \text{ for } k = 0, \pm 1, \pm 2, \dots \quad (5.24)$$

3) The cross-correlation $R_{xs}[k]$ based on the received hypothesis, is given by (5.25). Under H_1 (signal present), the cross-correlation becomes an autocorrelation of the transmitted preamble with a peak at $k = 0$. Alternatively, when the primary signal is idle and the gated signal represents only noise, it is cross-correlated with a preamble sequence resulting on no peaks. The overall detection procedure is illustrated in Figure 5.8.

$$R_{xs}[k] = \begin{cases} Re[\sum_{n=1}^{L} |g|^2 \mathrm{s}_{\mathrm{p}}\mathrm{s}^{*}{}_{\mathrm{p}}(n) + \sum_{n=1}^{L} n[n]\mathrm{s}^{*}{}_{\mathrm{p}}[n]] & : \ H_1 \\ Re\sum_{n=1}^{L} \mathrm{s}_{\mathrm{p}}[n]n^{*}[n] & : \ H_0 \end{cases} \quad (5.25)$$

which reduces to,

$$R_{xs}[k] = \begin{cases} |g|^2 \sum_{n=1}^{L} \left|\mathrm{s}_{\mathrm{p}}[n]\right|^2 + Re\sum_{n=1}^{L} \mathrm{s}_{\mathrm{p}}[n]n^{*}[n] & : \ H_1 \\ Re\sum_{n=1}^{L} \mathrm{s}_{\mathrm{p}}[n]n^{*}[n] & : \ H_0 \end{cases} \quad (5.26)$$

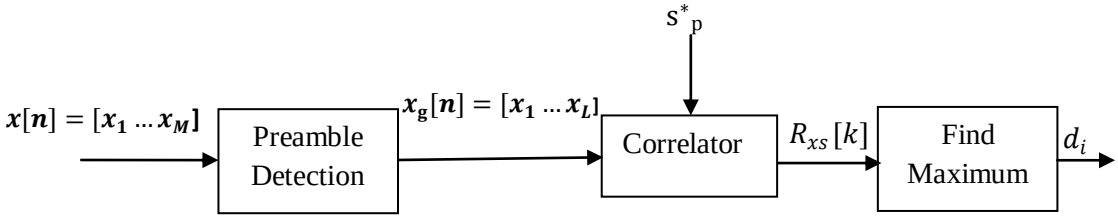

Figure 5.8. Coherent based feature extraction structure.

5.4 Numerical Results

Simulations were conducted to investigate the performance of parametric feature extraction techniques when applied to the proposed classifier model. Once again, the simulations are performed for both first and second order polynomial classifiers.

5.4.1 System Parameters

The simulation parameters considered for the primary signal, the fading channel, CR receivers and classifier parameters at the base station are presented as follows. The CR network consists of N CRs who provide the base station with features $\mathbf{d}$ in which a global decision is made, where $N \in \{1,3,5\}$ users. Signal models described in (5.16) and (5.17) are used to generate the transmitted primary signal. Due to simulation limitations in generating training and testing sequences, we considered a down scaled parameters for the primary signal that does not reflect practical applications. However, these parameters can be scaled up without affecting the performance if practical data are available. The simulated transmitted signal is a band-pass BPSK with data rate $R_b = 100$Kbps, carrier frequency $f_c = 5$MHz, and cyclic frequency $\alpha = 2f_c = 10$MHz. Whereas, the primary signal for coherent detection is a baseband BPSK with data rate $R_b = 100$Kpbs, frame length $M = 200$bits, and preamble sequence length $L \in \{16,32,40,48\}$ bits representing overhead percentages of $\frac{L}{M} \in \{8\%, 16\%, 20\%, 24\%\}$.

A flat slow Rayleigh fading channel is considered with coherence time $T_c = 20T_b$. The i^{th} CR receives a signal with signal-to-noise ratios SNR_i that follows a normal distribution with a variance $\sigma^2 = 4$ dB and mean equivalent to SNR_{avg}, emulating a log normally distributed loss path. The receiver's detector structure described in section 5.3 is used in the system simulation with the following parameters. The sampling frequency at the receivers is $f_s = 4f_{max}$, where $f_{\max} =$

$f_c + R_b$ satisfying the Nyquest sampling criterion. The observation window size for cyclostationary detector takes values of $M \in \{20,60,100,160,200\}$ bits. The spectral smoothing window $W(k)$ is chosen to be a central rectangular window. As per coherent detection, the receiver is assumed to acquire the gated signal based on the transmitted signal parameters mentioned above.

5.4.2 Simulation Results

In this section, we illustrate the results for the proposed classification system when cyclostationary features are fed to the CR base station for white spaces identification. In Figure 5.9, the achieved detection probability P_d is illustrated as the average received SNR at the secondary users' end is varied. We assume the distance between the CR network and the primary transmitted is very large; hence, the received SNR_{avg} is in the low SNR regime, i.e. $\text{SNR}_{\text{avg}} \leq 0$ dB. The decision threshold λ was computed during the validation stage of the classifier's design such that a target false alarm rate of 10% is achieved. The estimation of cyclostationary features was realized over an observation window with $M = 200$ bits. Note that we refer to cyclostationary feature detection with CFD and coherent detection with CD, in the obtained results.

The results obtained in Figure 5.9 present the performance improvement as the number of CRs cooperating in making the decision N increases. As N is increased from 1 receiver to 3 receivers, a gain of 4 dB is achieved at $P_d = 90\%$. However, performance improvements due to increasing cooperative CRs saturate for higher number of users. For instance, SNR_{avg} gain as N is raised from 1 to 3 is 4 dB and deteriorates to only 2 dB as N is raised from 3 to 5, at $P_d = 90\%$. Moreover, the results indicate that cyclostationary feature detection can be used for achieving at least 90% detection of received signals with SNR_{avg} of -18 dB with N =5. The performance of both linear and second order polynomial classifiers for different number of cooperating users is also shown in Figure 5.9. As in the case of nonparametric spectrum sensing, it is clear that as the order of classifier increases from first order to second order, no significant performance improvement is achieved.

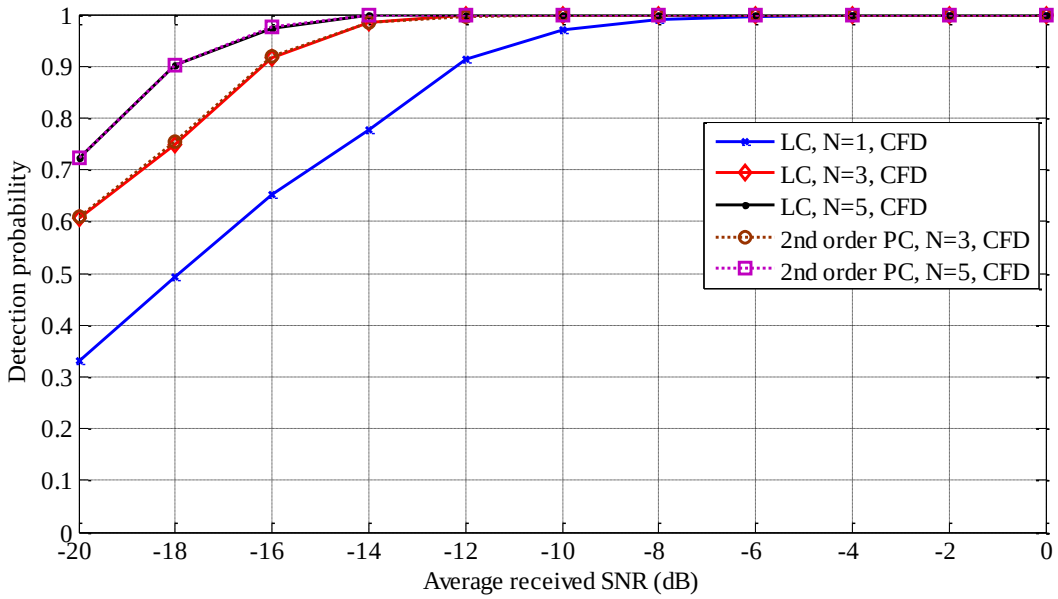

Figure 5.9. Detection performance of the proposed cooperative LC and 2nd order PC with CFD at $P_f = 10\%$ and observation window $M = 200$ bits.

Once again, the performance is improved by increasing the observation window size. The results of cyclostationary detection are illustrated in Figure 5.10, for linear and binomial classifiers at $\text{SNR}_{\text{avg}} = -14$ dB, $N = 3$ users, and $P_f = 10\%$. Further, to achieve at least 90% detection, a window of length 100 bits is needed. The performance can be improved to almost 99% detection if window size increases to 100 bits. Moreover, as the observation window size increases from $M = 20$ to $M = 200$ bits, probability of detecting received primary signal with $\text{SNR}_{\text{avg}} = -14$ dB increases from 73% to 98%.

To further illustrate detection performance of linear classifier, the ROC curve is obtained when primary signal is received with $\text{SNR}_{\text{avg}} = -14$ dB and observation window size of $M = 200$ bits. The ROC curves, given in Figure 5.11, show that the higher the number of cooperating radios is, the better the detection performance. For instance, maximum spectral utilization is achieved at $\text{SNR}_{\text{avg}} = -14$ dB with detection probabilities of 42%, 51%, and 86% when the number of cooperative CRs is 1, 3, and 5, respectively. Additionally, in order to maintain a minimum interference level with primary users, it is necessary to obtain high detection rate. A detection rate of 90% can be achieved at $\text{SNR}_{\text{avg}} = -14$ dB, while keeping a false alarm probability of 30%, 3%, and 0.9% with N=1, 3 and 5, respectively.

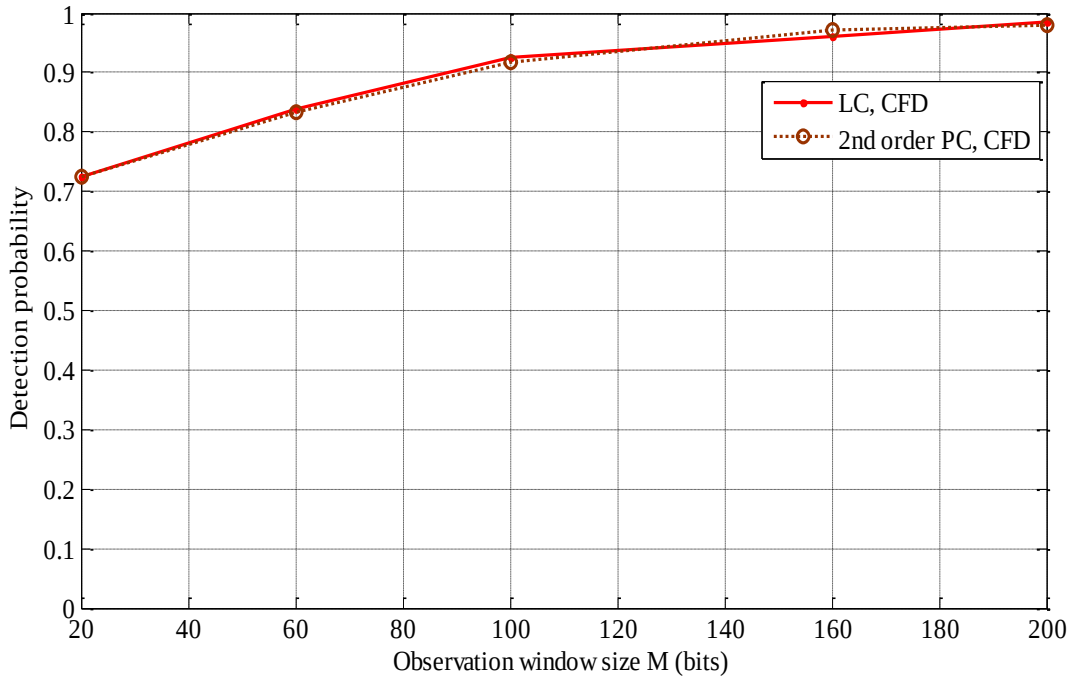

Figure 5.10. Detection performance of cooperative LC and 2nd order PC with CFD as M is varied at $\text{SNR}_{\text{avg}} = -14$ dB, $N = 3$ users, and $P_f = 10\%$.

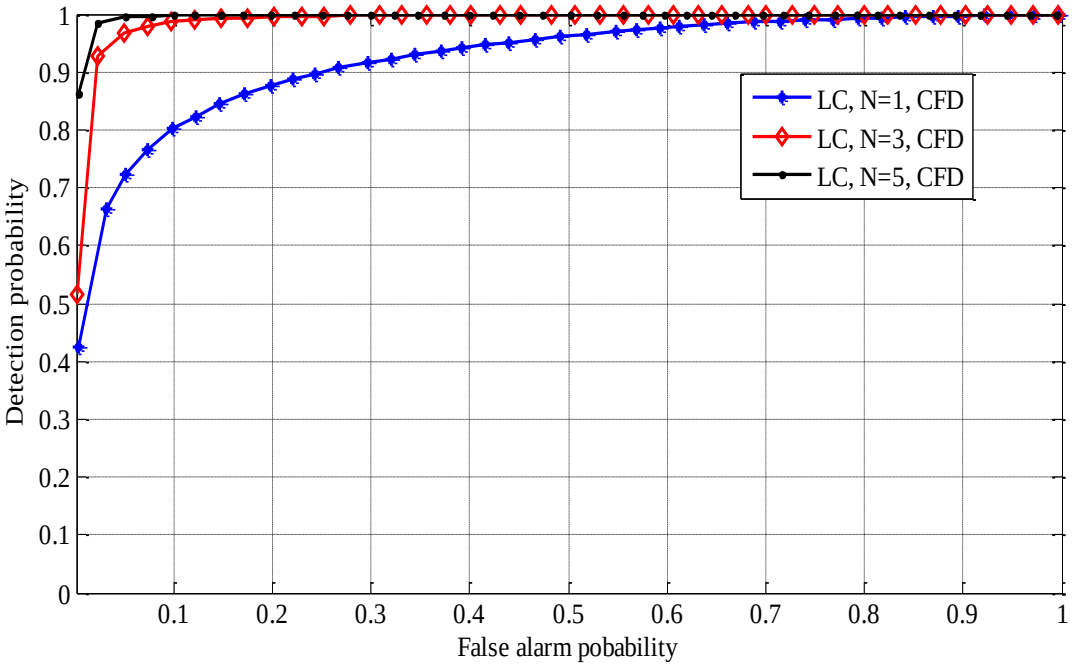

Figure 5.11. The ROC curves of the proposed LC with CFD at $\text{SNR}_{\text{avg}} = -14$ dB and $M = 200$ bits.

Simulations were conducted using coherent detection to provide features to the designed classification system. Figure 5.12 shows the obtained detection probability P_d as the received primary signal's level is varied. The system is evaluated after training the designed classifier to achieve false alarm probability of 10%. Coherent detection was implemented for primary signal with preamble size of $L = 16$bits and frame length of $M = 200$bits. At a detection rate of $P_d = 90\%$, a gain of around 6 dB can be realized as N increases from 1 to 3. The achieved gain; however, becomes around 1.5 dB as N increases from 3 to 5. It is evident from Figure 5.12 that coherent detection provides reliable signal identification with $P_d > 98\%$, when the received signal level is above -10 dB and $N = 5$. Moreover, both linear and second order polynomial classifier perform comparably as coherent detection is utilized in feature extraction.

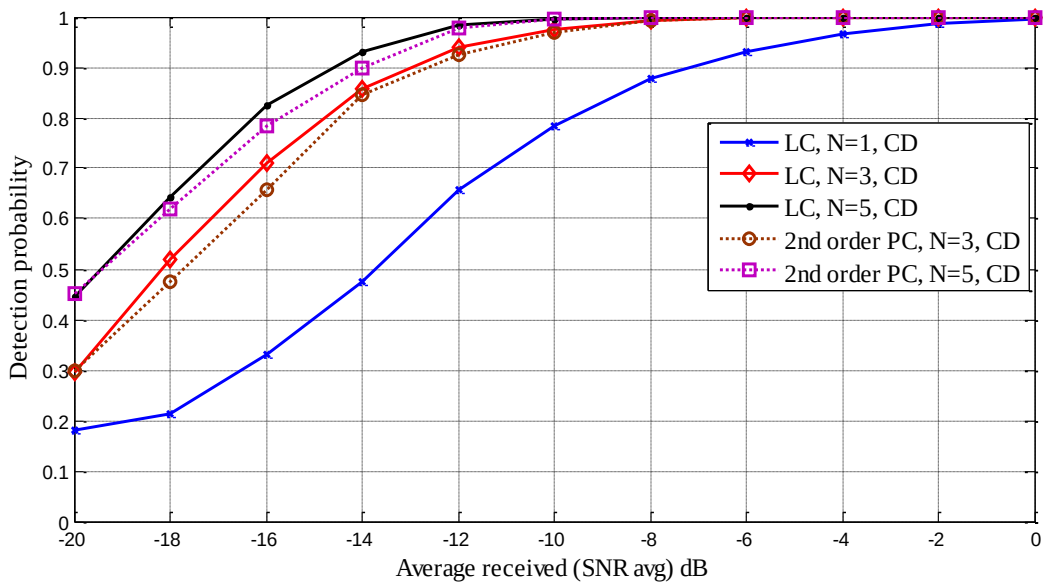

Figure 5.12. Detection performance of the proposed cooperative LC and 2nd order PC with CD at $P_f = 10\%$ and $L = 16$ bits.

The ROC curve for coherent detection based sensing for various numbers of cooperative CRs and a received signal level of -14 dB is demonstrated in Figure 5.13. We consider a primary signal with same parameter of $M = 200$ and $L = 16$ bits. It is apparent that there is a performance variation as different number of CRs collaborates in making the decision. The performance gap between various numbers of CRs shrinks, as the false alarm probability increases.

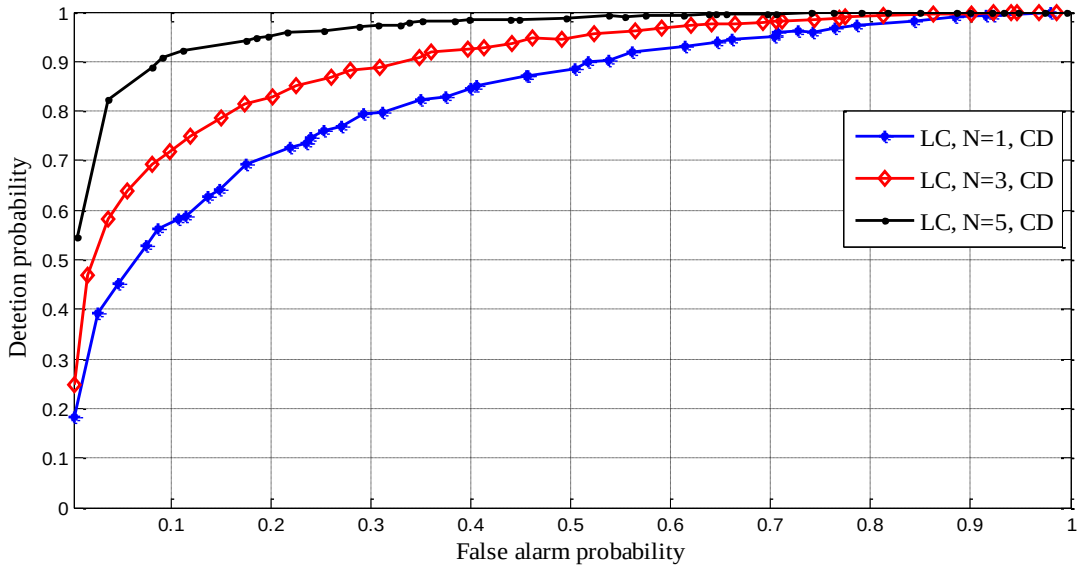

Figure 5.13. The ROC curves of the proposed LC with CD at $\mathrm{SNR}_{\mathrm{avg}} = -14$ dB and $L = 16$ bits.

Finally, we investigate the performance gain achieved as the length of preamble sequence, utilized in coherent detection, increases. The effect of increasing the preamble length on the classification system performance can be examined by the aid of Figure 5.14. The figure presents the $\mathrm{SNR}_{\mathrm{avg}}$ required to obtain a specific detection probability and false alarm rate, as the preamble length increases. Longer preamble sequences result in higher gain in $\mathrm{SNR}_{\mathrm{avg}}$. In other words, a lower level of received primary signal is sufficient to achieve a certain detection rate as preamble length is increased. For example, a signal level of -16 dB is sufficient to obtain $P_d = 90\%$ for $L = 40$, while a signal level of -17 dB is required for $L = 50$. This results in a SNR gain of around 1 dB.

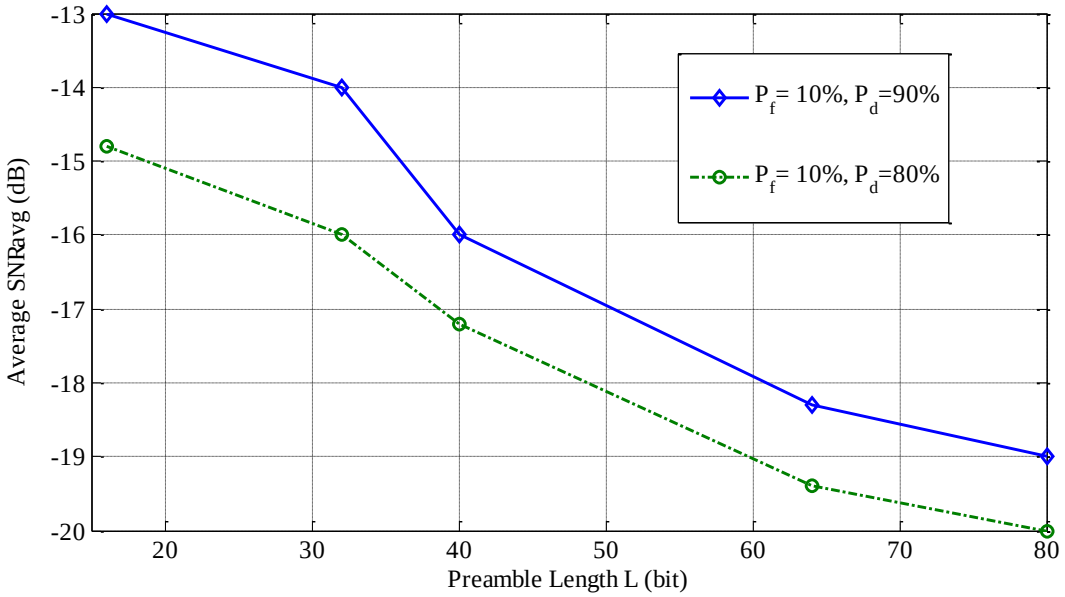

Figure 5.14. SNR gain as received preamble lengths varies.

5.5 Discussion of Results

In this section, the obtained results of parametric sensing schemes are discussed. The results demonstrate the reliable performance of cyclostationary detection. For instance, it provides a 100% detection rate at SNR_{avg} above -12 dB, and can be maintained above 90% for smaller values of SNR_{avg} . A reliable detection of primary transmission is very useful in CR networks as the level of the received signal by a CR could be very low due to physical proximity or shadowing effect. Hence, having a relatively high detection probability provides better performance in terms of interference avoidance with primary users for a specific false alarm probability.

A comparison of the performance of cyclostationary and coherent based feature extraction techniques is shown in Table 5.1 and Table 5.2. Results indicate the superior performance of cyclostationary detection over coherent detection in terms of detection probability at a given false alarm rate. This suggests that detection of cyclic features present in a signal is more reliable than coherent detection of synchronization preamble sequences. However, the number of samples used to coherently detect preamble transmission, i.e. preamble sequence length L, is relatively short when compared to a full frame M used to estimate the cyclic features. Note that in both detection schemes secondary users need to wait for a full frame of M bits to make a

decision; however, in coherent detection only L bits are utilized in making the decision. Consequently, the longer the preamble sequence is, a better performance is achieved; however, a longer transmission overhead is needed, lowering the spectral efficiency of primary users. Moreover, cyclostationary detection is capable of providing high detection probability with higher spectral utilization, when compared to coherent detection. As high spectral utilization is required, referring to low false alarm rate, a considerable degradation in detection probability is observed in coherent detection as shown in Table 5.2.

Table 5.1. Detection probability of CD and CFD at $P_f = 10\%$ with various number of receivers and different SNR.

		SNR $= 0$ dB		SNR $= -10$ dB		SNR $= -20$ dB	
		$N = 3$	$N = 5$	$N = 3$	$N = 5$	$N = 3$	$N = 5$
Detection Probability	Cyclostationary	100%	100%	100%	100%	60%	72%
	Coherent	100%	100%	97.5%	99.6%	29.5%	44.5%

Table 5.2. Detection probability of CD and CFD at SNR $= -14$ dB with various number of receivers and different P_f.

		$P_f = 1\%$		$P_f = 10\%$		$P_f = 20\%$	
		$N = 3$	$N = 5$	$N = 3$	$N = 5$	$N = 3$	$N = 5$
Detection probability	Cyclostationary	70.97%	92.56%	98.4%	99.86%	100%	100%
	Coherent	41%	63.5%	85.7%	93.2%	82.7%	95.2%

The effect of window size used in cyclostationary detection is studied. The performance improvement achieved by varying observation window size is illustrated in Figure 5.10. However, there is an upper limit on the improvement in detection rate at which increasing observation window length no longer improves detection probability with a specific constraint on false alarm rate and SNR_{avg} level. Observation window length can be optimized to achieve maximum detection

probability at a received signal SNR_{avg} level. This suggests utilizing shorter sensing windows, as a high signal level is received so that faster decisions are made with high detection probability, and vice versa.

Furthermore, having the nonparametric schemes analyzed and evaluated, we provide a comprehensive performance evaluation of parametric feature extraction techniques as compared to nonparametric ones in terms of different performance metrics as follows:

- In terms of detection performance at different SNR values, parametric sensing provides high detection probabilities at very small SNR values as compared to nonparametric schemes. Moreover, the detection performance of parametric schemes at very small false alarm rates is considerably enhanced, relative to nonparametric schemes.
- Among all schemes, cyclostationary feature detection provides the best performance in terms of both detection and false alarm rates. On the other hand, coherent detection with preamble overhead of 8%, provides slightly lower performance than that of autocorrelation detection. Energy detection constitutes the poorest performance among all studied techniques.
- Cyclostationary feature detection represents the optimal feature extraction scheme, if information on primary signal is available. The implementation of cyclostationary feature detection relies on the knowledge of carrier frequency and modulation type of the primary signal. The obvious drawback of cyclostationary detection is the high computational complexity required to extract cyclic features at CRs, as compared to other techniques. On the other hand, it provides high reliability to the CR network under low SNR conditions.
- Coherent and autocorrelation based feature extraction perform comparably in terms of detection at different SNR levels. However, the fairness of this comparison is doubtful since the correlation computations are performed over small number of samples in coherent detection, represented by the preamble length. On the other hand, autocorrelation estimation is performed over the length of a full frame, providing longer estimation time and higher complexity. Once again, coherent detection requires

knowledge of preamble sequences utilized by primary users, relative to autocorrelation detection that does not rely on any prior information.

- Finally, energy detection represents the feature extraction scheme with least detection capability under very low SNR, since the energy content of the received signal is highly susceptible to noise and fading conditions. However, energy detection represents an attractive detection technique under high SNR regimes for its simplicity and minimum a prior information requirements.

A comparison of the studied feature extraction techniques is illustrated in Table 5.3.

Table 5.3. Comparison of parametric and nonparametric feature extraction schemes.

	Prior information	Complexity	Detection Performance
Energy	Not required	Low	Poor
Autocorrelation	Not required	Medium	Good
Cyclostationary	Modulation type and carrier frequency	High	Excellent
Coherent	Preamble or other synchronization sequences	Medium	Good

5.6 Conclusions

In this chapter, the problem of parametric based signal detection and classification has been tackled. The performance of both cyclostationary and coherent based feature extraction techniques is simulated and analyzed. The presented results justify the capability of the proposed pattern recognition system to detect presence of primary signals. We also illustrated the power of cooperative spectrum sensing as opposed to sensing based on single CR.

The performance of parametric and nonparametric spectrum sensing schemes was also compared. The potential of the proposed classification scheme is supported with the great performance in detection probabilities at very low average SNR values for

both schemes. Simulation results have demonstrated the substantial improvement provided by parametric spectrum sensing techniques, especially cyclostationary detection, over the nonparametric in terms of different performance measures.

CHAPTER 6

CONCLUSIONS AND FUTURE WORK

6.1 Conclusions

The deployment of cognitive radio networks has been proposed to overcome the radio spectrum scarcity problem that poses a limitation to the development of wireless communication applications. Dynamic spectrum allocation is facilitated through CR networks in which spectrum holes are detected and opportunistically utilized by the CR users. However, secondary users in a CR network are required to maximally exploit frequency bands when licensed users are idle, yet keeping a minimum interference level to the primary network. Consequently, spectrum sensing has become an essential functionality of CRs, in order to inhibit harmful interference to primary users and utilize available spectral opportunities. This fact has motivated the research in developing efficient and reliable spectrum sensing techniques.

Pattern recognition models were proposed in this work to tackle the problem of spectrum sensing in CR networks. The proposed classifier model is based on cooperative sensing, in which secondary users monitor channel usage in a given area and cooperate through a centralized node to provide the channel information. Collaborative spectrum sensing provides spatial diversity to overcome shadowing and fading impacts of the surrounding environment. The cooperation between secondary users was achieved through a classification model that utilizes input features by collaborative users to provide an output decision on the availability of the spectrum. First and second order polynomial classifiers were modeled, trained, validated and evaluated as the classifier models. Our simulation results indicate that first order polynomial classifier is an attractive model since it provides the same performance as second order classifiers with reduced complexity.

Various spectrum sensing techniques were adopted for the feature extraction stage of the proposed classification system. Nonparametric spectrum sensing schemes were implemented including energy based and autocorrelation based feature extraction, in which secondary users require no a priori knowledge of primary signal characteristics. Furthermore, parametric spectrum sensing schemes, such as cyclostationary based and coherent based feature extraction were investigated where signal detection is dependent on available information on primary user signal, including carrier frequency and synchronization preambles.

The performance of the above feature extraction schemes was evaluated in terms of detection probability under different received SNR levels and various target false alarm rates. Results demonstrated that cyclostationary detection constitutes a prominent candidate for feature extraction when information on primary signal is available, since it outperforms coherent detection substantially. However, the remarkable detection capability of cyclostationary detection is achieved at the expense of higher implementation complexity. Additionally, autocorrelation detection yields a superior performance over energy detection, especially for small received signal levels. However, the basic advantage of energy detection over autocorrelation detection is its lower computational complexity. Furthermore, the advantages of utilizing spatial diversity, via cooperative sensing, in enhancing the detection probability were illustrated.

The impact of observation window size over which features are extracted has been studied. It has been shown that, longer sensing time can improve the detection performance considerably for energy based and cyclostationary based feature extraction. Detection improvement due to increasing sensing time is achieved at the expense of lowering the network's agility, since longer time is required to decide on the vacancy of the spectrum. The performance of coherent based feature extraction has shown susceptibility to synchronizing sequence length. Though longer preamble sequence results in a high detection performance at the CR network end, it considerably lowers transmission efficiency of primary user due to the large transmission overhead.

6.2 Future Work

In this thesis, a solution for the problem of cooperative spectrum sensing in CR networks is attempted through the design of a pattern recognition model, which effectively offers a soft fusing rule. We have implemented several detection techniques utilized in spectrum sensing in a single cell CR network; where we mainly assumed simple modulation schemes for the primary signal model. Moreover, the designed system assumed each secondary user receives a single path from the primary user under flat fading conditions. This basically suggests that there is definitely a room to further improve the classification based spectrum sensing system in environments with frequency selective fading, in which a multiple cellular CR network is operating. In this section, various areas that could be addressed to improve the classification spectrum sensing are highlighted:

Spectrum sensing for different modulation schemes for the primary signal model needs to be investigated. As specified by the IEEE802.22 Working Group, CR networks are envisioned to be operating in VHF and UHF (54–862 MHz) bands that are currently allocated for analog and digital television (TV) broadcasting and low-power licensed devices like wireless microphones [2]. Moreover, spectrum sensing of primary signals employing adaptive modulation schemes could also be investigated.

It is also suggested to examine the performance of the developed polynomial classifier system under frequency selective fading channels. We can overcome the effect of frequency selective fading channel through the use of frequency diversity, in which sensing is performed over a number of discrete spectral frequencies. The decision may be then performed via combining features at the selected frequencies. Furthermore, different models for large scale fading could be examined where larger variations of SNR at different cognitive are assumed. In this case, the diversity gain may be more noticeable due to the larger spread in SNR distribution for different users.

Multiple cellular CR networks could be studied in which spectrum sensing would be designed for the whole network. The information from different CR cells may be combined using the proposed classifier model to decide on the vacant spectrum. In such scenarios, channel and power allocation needs to be addressed for providing efficient network resource allocation.

REFERENCES

[1] M. Naraghi and T. Ikuma, "Autocorrelation-based spectrum sensing for cognitive radios," *IEEE Trans. On Vehicular Technology*, vol. 59, pp. 718-733, February, 2010.

[2] C. Cordeiro, K. Challpali, and D. Birru, "IEEE 802.22: An introduction to the first wireless standard based on cognitive radios", *Journal of communications, vol.1*, pp.38-47, 2006.

[3] F. Granelli, et al., " Standardization and research in cognitive and dynamic spectrum access networks: IEEE SCC41 efforts and other activities," IEEE Communications Magazine, pp. 71-78, January, 2010.

[4] N. Devroye, M. Vu, and V. Tarokh "Cognitive radio networks", IEEE Signal Processing Magazine, pp. 12-23, November, 2008.

[5] Unlicensed Operation in the TV Broadcast Bands; Additional Spectrum for Unlicensed Devices Below 900 MHz and in the 3 GHz Band, FCC-04-113, Fed. Commun. Commission, Washington, DC, Nov, 2004.

[6] E. Hossain and V. K. Bhrgava, *Cognitive Wireless Communication Network*, 1st ed. Springer, 2007.

[7] Z. Quan,, S. Cui, and A. H. Sayed, "Optimal linear cooperation for spectrum sensing in cognitive radio networks," *IEEE Journal of Selected Topics In Signal Processing*, vol.2, pp.23 -40, 2008.

[8] T. Yucek and H. Arslan, "A survey of spectrum sensing algorithms for cognitive radio applications," *IEEE Communications Surveys & Tutorials*, vol.11, pp.116 -130, 2009.

[9] D. Cabric, A. Tkachenko, and R. Brodersen, "Spectrum sensing measurements of pilot, energy, and collaborative detection," *in Proc. IEEE Military Commun. Conf*, 2006, pp. 1–7.

[10] T. Y¨ucek and H. Arslan, "Spectrum characterization for opportunistic cognitive radio systems," *in Proc. IEEE Military Commun. Conf*., 2006, pp. 1–6.

[11] N. Khambekar, C. Spooner, and V. Chaudhary, "Listen-While-Talking: A techniques for primary user protection", *in Proc. Wireless Communications and Networking*, Budapest, Hungary, 2009, pp. 1-5.

[12] N. Khambekar, L. Dong and V. Chaudhary, "Utilizing OFDM guard interval for spectrum sensing," Wireless Communications and Networking, 2007, pp. 38-42.

[13] P.D.Sutton, K.E. Nolan, and L.E. Doyle, "Cyclostationary signature in practical cognitive radio applications," *IEEE Journal of Selected areas in communications*, vol. 26, pp. 13 -24, 2008.

[14] D. Cabric, A. Tkachneko, and R.W. Brodersen, "Experimental study of spectrum sensing based on energy detection and network cooperation," Berkeley Wireless Research Center, Berkeley, USA, Tech. Rep. 916-1010-BB, 1997.

[15] A. GHasemi and E.S. Sousa, "Collaborative spectrum sensing for opportunistic access in fading environments", *in First IEEE International Symposium*, 2005, pp. 131-136.

[16] F. F. Digham, M. Alouini, and Marvin K. Simon, "On the energy detection of unknown signals over fading channels", IEEE *Trans. on Communications* vol. 55, pp. 21-24, 2007.

[17] T. Zhang, G. Yu, and C. Sun," Performance of cyclostationary features based spectrum sensing method in a multiple antenna cognitive radio sensing," *in Prec of Wireless Communications and Networking Conference*, 2009, pp. 1-5.

[18] D. Cabric, S. Mishra, and R. Brodersen, "Implementation issues in spectrum sensing for cognitive radios," *in Proc. Asilomar Conf. on Signals, Systems and Computers*, vol. 1, 2004, pp. 772–776.

[19] G. Vardoulias, J. Faroughi-Esfahani, G. Clemo, and R. Haines, "Blind radio access technology discovery and monitoring for software defined radio communication systems: Problems and techniques," *in Proc. Int. Conf. 3G Mobile Communication Technologies*, 2001, pp. 306–310.

[20] S. Shankar, C. Cordeiro, and K. Challapali, "Spectrum agile radios: Utilization and sensing architectures," *in Proc. IEEE Int. Symposium on New Frontiers in Dynamic Spectrum Access Networks*, 2009, pp. 160–169.

[21] Agrawal, D. and Zeng, Q., *Introduction to Wireless and Mobile Systems*, 2nd edition, Thomson, Canada, 2006.

[22] Medeisis, A. and Kajackas, A., "On the use of the universal Okumura-Hata propagation prediction model in rural areas", *in Proceeding of Vehicular Technology Conference*, 2000, pp. 1815-1818.

[23] Mark, J. and Zhuang W., *Wireless Communications and Networking*, Prentice Hall, New Jersey, 2003.

[24] K. Kim, I.A. Akbar, K. k. Bau, J. Um, C.M. Spooner, and J. H. Reed, " Cyclostationary approaches to signal detection and classification in cognitive radio," *in Proceedings of 2nd IEEE international symposium on*, 2007, pp. 212-215.

[25] K. Assaleh, K. Farrel, and R. J. Mammone, " A new method of modulation classification for digitally modulated signals", *in IEEE Military Comm Conf*, vol. 2, 1992, pp. 712-716

[26] S. Theodoridis and K. Koutroumbas, *Pattern Recognition*, 3rd ed. San Diego: Academic Press, 2006.

[27] S.Haykin , *Neural Networks and Learning Machines*, 3rd ed. New Jersey: Academic Press, 2009.

[28] P.T. Boufounos, "Signal processing for DNA sequencing" Ms.c. Thesis, Massachusetts Institute of Technology, Massachusetts, USA, 2002.

[29] M. Khasawneh, K. assaleh, W. Sweidan and M. Haddad, "The application of polynomial discriminant function classifiers to isolated Arabic speech recognition," *in Proc. IEEE Int. Conf on Neural Networks*, 2004, pp. 3077–3081.

[30] W.M. Campbell, K.T. Assaleh, and C.C. Broun, "Speaker recognition with polynomial classifiers", *IEEE Trans. on Speech and Audio Processing*, vol. 10, pp. 205-212, 2002.

[31] D. Srinivasan and V. Sharma, "A reduced multivariate polynomial based neural network model pattern classifier for freeway incident detection," *in Proc. Int. Conf on Neural Networks*, 2007, pp. 12–17.

[32] D. F. Specht, “Generation of polynomial discriminant functions for pattern recognition”, *IEEE Trans. on Electronic Computers*, vol. 16, pp. 308-319, 1967.

[33] B, Wang, "Dynamic Spectrum Allocation and Sharing in Cognitive Cooperative Networks" Ph.D. Dissertation, University of Maryland, Maryland, USA, 2009.

[34] J. Proakis and M. Salehi, *Digital Communications*, 5th ed. McGraw-Hill, 2008.

[35] W. A. Gardner, *Cyclostationarity In Communications and Signal Processing*, 1st ed. NY: IEEE Press, 1994.

[36] W. A. Gardner, "Exploitation of spectral redundancy in cyclostationary in signal", IEEE Signal Processing Magazine, pp. 15-35, 1991.

[37] H. Bolcskei, “Blind estimation of symbol timing and carrier frequency offset in wireless OFDM systems,” *Communications, IEEE Transactions on*, vol. 49, pp. 988–999, 2001.

[38] J. Heath, R.W. and G. Giannakis, “Exploiting input cyclostationarity for blind channel identification in OFDM systems", *IEEE Transactions on Signal Processing*, vol. 47, pp. 848–856, 1999.

[39] Y. Lin and C. He, "Subsection-Average cyclostationary feature detection in cognitive radio," *in IEEE Int. Conf on Neural Networks & Signal Processing*, 2008, pp. 604-608.

[40] S. McBeath, J. Smith, L. Chen, and A. S. Sean, " VoIP support using group resource allocation based on the UMB system ", IEEE Communications Magazine, pp. 15-35, 2009.

VITA

Yasmin Adel Hassan was born on September 7, 1986, in Kingdom of Saudi Arabia. She lived in Egypt and then moved to the United Arabs Emirates in 2000, where she joined a local public school and graduated from Zabeel High School in 2003, holding the first rank among Emirati schools. She received a Scholarship from the ruler of Sharjah to the American University of Sharjah, UAE, from which she graduated suma cum laude, in 2008. Her degree was a Bachelor of Science in Electrical Engineering. Directly after her Bachelors, Yasmin Adel began a master's program in Electrical Engineering at the American University of Sharjah in 2008. She worked as a graduate teaching assistant for two years during her master's study. Ms. Adel was awarded the Master of Science degree in Electrical Engineering in 2010.